

Administration of Ricin Induces a Severe Inflammatory Response via Nonredundant Stimulation of ERK, JNK, and P38 MAPK and Provides a Mouse Model of Hemolytic Uremic Syndrome

Veselina Korcheva,* John Wong,*
Christopher Corless,[†] Mihail Iordanov,* and
Bruce Magun*

From the Departments of Cell and Developmental Biology* and
Pathology,[†] Oregon Health and Science University,
Portland, Oregon

Recent interest in the health consequences of ricin as a weapon of terrorism has led us to investigate the effects of ricin on cells *in vitro* and in mice. Our previous studies showed that depurination of the 28S rRNA by ricin results in the inhibition of translation and the coordinate activation of the stress-activated protein kinases JNK and p38 MAPK. In RAW 264.7 macrophages, ricin induced the activation of ERK, JNK, and p38 MAPK, the accumulation of mRNA encoding tumor necrosis factor (TNF)- α , interleukin (IL)-1, the transcription factors c-Fos, c-Jun, and EGR1, and the appearance of TNF- α protein in the culture medium. Using specific inhibitors of MAPKs, we demonstrated the nonredundant roles of the individual MAPKs in mediating proinflammatory gene activation in response to ricin. Similarly, the intravenous administration of ricin to mice led to the activation of ERK, JNK, and p38 MAPK in the kidneys, and increases in plasma-borne TNF- α , IL-1 β , and IL-6. Ricin-injected mice developed the hallmarks of hemolytic uremic syndrome, including thrombotic microangiopathy, hemolytic anemia, thrombocytopenia, and acute renal failure. Microarray analyses demonstrated a massive proinflammatory transcriptional response in the kidneys, coincidental with the symptoms of hemolytic uremic syndrome. Therapeutic management of the inflammatory response may affect the outcome of intoxication by ricin. (*Am J Pathol* 2005, 166:323–339)

In view of its wide availability and ease of purification, ricin has been used as a toxic and lethal agent by totalitarian regimes and, recently, by terrorist groups.¹ In humans, the estimated lethal dose of ricin is 1 to 10 μ g per kg of body weight.² The majority of described cases of ricin intoxication has resulted from the ingestion of castor beans and is manifested by hemorrhagic diarrhea, liver necrosis, diffuse nephritis, and splenitis.¹ One of the few described cases of ricin injection was the political assassination of the noted Bulgarian dissident Georgi Markov³ whose body was penetrated by a ricin-containing pellet. Before his death, which occurred 3 days later, he developed fever, lymphadenopathy near the site of inoculation, hypotension with vascular collapse, and shock.³ Although the toxicity of ricin varies according to the route of administration, the clinical symptoms frequently are related to a severe inflammatory response and multiorgan failure.

Ricin is a member of a family of protein toxins whose cytosolic target is the 28S rRNA of the 60S ribosomal subunit.⁴ The cytotoxicity of ricin results from the depurination of the 28S rRNA at a single adenine nucleotide (A4565 in humans and A4256 in mouse) with consequent inhibition of protein translation. The depurination of 28S rRNA by ricin also initiates the ribotoxic stress response, characterized by activation of the stress-activated protein kinases (SAPKs), N-terminal-c-Jun-kinases (JNK), and p38 MAPK, via the activation of kinases situated upstream.^{5–9} Activation of the SAPK cascade is known to modulate the expression of a variety of genes that encode proinflammatory cytokines and chemokines.^{10,11}

Supported by the National Institutes of Health (grants ES889456 and AI1059335).

Accepted for publication October 1, 2004.

Address reprint requests to Bruce Magun, Oregon Health and Science University, 3181 SW Sam Jackson Park Rd., Portland, OR 97239. E-mail: magunb@ohsu.edu.

The inflammation and failure of multiple organs related to the toxicity of ricin have been evaluated in different experimental models. In 1987 Bingen and colleagues¹² confirmed the ability of ricin, delivered intravenously into rats, to cause diffuse endothelial cell damage and formation of thrombi within the liver microvasculature, followed by liver necrosis. Taylor and colleagues¹³ described a rat model of ricin-induced hemolytic uremic syndrome (HUS) that recapitulates most of the hallmarks of Shiga toxin (Stx)-associated HUS in humans. These features include extensive thrombotic microangiopathy, hemolytic anemia, thrombocytopenia, and acute renal failure.^{14–17} Both ricin and Stx act to deplete the same adenine within the ricin/sarcin loop of eukaryotic mammalian 28S rRNA.¹⁸ Each toxin consists of A and B subunits, of which the B subunits determine the binding to cell surfaces. Whereas ricin binds to galactose residues,¹⁹ Stx binds to cell surfaces via a glycosphingolipid receptor, Gb3.²⁰ After endocytosis and retrograde transport through the Golgi apparatus, the A subunits of each toxin enter the cytosol where they depurinate 28S rRNA, thereby inhibiting protein synthesis²¹ and activating the SAPK cascade.⁵

HUS is a major cause of acute renal failure in children in North America.^{22,23} Abundant evidence supports the conclusion that diarrhea-associated HUS involves an acute inflammatory response, the extent of which is a predictor of the clinical outcome. Patients with HUS display markedly elevated proinflammatory cytokines such as tumor necrosis factor (TNF)- α , interleukin (IL)-1 β , and chemokines such as monocyte chemoattractant protein-1 (MCP-1), IL-8, growth related oncogene (Gro)- α and - γ .^{15,17,24–26}

The availability of suitable experimental animal models of HUS could provide insight into the molecular mechanisms and sequence of events that occur in HUS. However, the distribution of Gb3 receptors for Stx on cell types varies widely among species, and it has been suggested that these differences may account for the inability of Stx to recapitulate the hallmarks of the human HUS in the available animal models.¹³ To bypass the restricted distribution of Stx receptors, Taylor and colleagues¹³ administered ricin, which, unlike Stx, was able to recapitulate many of the features of HUS in rats.

An additional rationale for elucidating the mechanisms responsible for ricin's toxicity relates to the administration of ricin as an immunotoxin in the therapy of hematological malignancies and solid tumors.^{27–29} The dose-limiting side effect of many of the ricin-containing immunotoxins that have been applied in clinical trials is the appearance of vascular leak syndrome,²⁷ whose main feature is the altered integrity of the vascular endothelial cells. Although the cause of endothelial cell damage remains unknown, it has been suggested that the direct uptake of ricin by the endothelial cells and macrophages constitutes the triggering event in vascular leak syndrome pathogenesis.²⁸

In this study, we have demonstrated that ricin activates members of the MAPK family, induces the expression of proinflammatory genes *in vitro*, and causes a severe inflammatory response *in vivo*. The *in vitro* activation of a variety of proinflammatory mediators by ricin requires the

activation of ERK1/2, JNK, and p38 MAPK. We have shown that after the intravenous administration of ricin, mice developed a syndrome that shared most of the characteristics of human HUS, including thrombocytopenia, hemolytic anemia, renal failure, and microvascular thrombosis.

Materials and Methods

Mice

C57BL/6J mice were purchased from The Jackson Laboratory, Bar Harbor, ME. Male mice 8 to 10 weeks of age and weighing 18 to 24 g were used throughout the experiments. Mice were housed under 12-hour light-dark cycle and fed with standard diet *ad libitum*. To collect 24-hour diuresis, mice were housed for 24 hours in diuresis metabolic cages (model M-D-METAB; Nalgene, Braintree, MA) provided with grounded standard diet *ad libitum*. Before experimental procedures, mice were anesthetized intraperitoneally with 80 mg/kg of ketamine and 10 mg/kg of xylazine. All of the animal procedures were performed according to protocols that have been approved by the Institutional Animal Care and Use Committee at Oregon Health and Science University, Portland, OR.

Cell Lines

The murine macrophage cell line RAW 264.7 was purchased from the American Type Culture Collection (Rockville, MD) and maintained in Dulbecco's modified Eagle's medium (DMEM; Life Technologies, Inc., Grand Island, NY) supplemented with gentamicin (50 μ g/ml) and 10% fetal bovine serum (Cellgro, Herndon, VA) at 37°C in humidified CO₂. RAW 264.7 cells were plated into 6- and 10-cm tissue culture plates (Sarstedt, NC) at a concentration of 5.0×10^6 and 8.0×10^6 cells, respectively. Before experiments, cells were incubated in serum-free DMEM for 2 hours. The human macrophage cell line THP-1 was obtained from American Type Culture Collection and maintained in RPMI 1640 medium (Cellgro) supplemented with 50 μ g/ml of gentamicin and 10% fetal bovine serum. THP-1 cells were plated in 10-cm tissue culture dishes at a concentration of 8.0×10^6 cells and were differentiated in the presence of 0.1 μ mol/L 12-O-tetradecanoylphorbol 13-acetate (Sigma-Aldrich, St. Louis, MO) for 72 hours. Before experiments, cells were incubated in serum-free RPMI 1640 for 2 hours.

Reagents and Antibodies

Ricin was purchased from Vector Laboratories, Burlingame, CA. Lipopolysaccharide (LPS), derived from *Escherichia coli* O111:B4, was obtained from Sigma-Aldrich. The MAP kinase inhibitors UO126, SP600125, and SB203580 were obtained from Calbiochem, La Jolla, CA. The mouse TNF- α enzyme-linked immunosorbent assay (ELISA) Ready-SET-Go was purchased from eBioscience (catalog no. 88-7324-76), San Diego, CA; the mouse IL-6

immunoassay kit was obtained from R&D Systems (catalog no. M6000), Minneapolis, MN; the mouse IL-1 β ELISA kit was purchased from BD Bioscience (catalog no. 559603), San Diego, CA. Antibodies against phospho-JNK, phospho-p38, and phospho-ERK1/2, were purchased from Cell Signaling Technology, Beverly, MA; antibody against p38 was obtained from Santa Cruz Biotechnology, Santa Cruz, CA; rabbit polyclonal antibody against mouse fibrin(ogen) was purchased from Nordic Immunology, Tilburg, The Netherlands; and horseradish peroxidase-conjugated antibody was obtained from Vector Laboratories.

Measurement of Protein Synthesis

RAW 264.7 cells were grown in 12-well tissue culture dishes in 10% fetal bovine serum-DMEM. Before the treatments with ricin, the cells were serum-deprived for 2 hours. Two and a half hours after the addition of ricin, the cells were pulsed-labeled for 30 minutes with 2 μ Ci of [3 H]-leucine in 0.3 ml of serum-free DMEM. The incorporation of leucine was stopped by the addition of 10% trichloroacetic acid. Cells were washed 3 \times with 5% trichloroacetic acid, followed by 88% formic acid to solubilize the trichloroacetic acid-insoluble proteins, and the samples were counted in a scintillation counter. To determine a suitable background for the assay, untreated cells were maintained on ice for 15 minutes, before pulse-labeling on ice for 30 minutes with 2 μ Ci of [3 H]-leucine in 0.3 ml of serum-free DMEM. The reaction was stopped by the addition of 10% trichloroacetic acid, after which samples were further processed as described above.

Immunoblot Analyses

RAW 264.7 cells cultured in 6-cm tissue culture dishes were lysed in 250 μ l of 2 \times sodium dodecyl sulfate-polyacrylamide gel electrophoresis (SDS-PAGE) loading buffer and boiled for 1 minute. The lysates were separated via 10% SDS-PAGE, transferred to a polyvinylidene difluoride membrane (Millipore, Bedford, MA), and probed with the corresponding primary antibodies. For the immunoblot analyses performed on mouse tissue, the whole kidneys were homogenized in lysis buffer (20 mmol/L Tris-HCl, pH 7.5, 140 mmol/L NaCl, 1 mmol/L EDTA, 1 mmol/L EGTA, 1% Triton X-100, 2.5 mmol/L Na $_4$ P $_2$ O $_7$, 1 mmol/L C $_3$ H $_7$ O $_6$ PNa $_2$, 1 mmol/L Na $_3$ VO $_4$, 10 mmol/L NaF, 1 \times Protease inhibitors cocktail; Roche Applied Science, Indianapolis, IN). After incubation for 10 minutes at 4°C, the lysates were centrifuged at 4°C for 10 minutes at 10,000 $\times g$. The protein concentration of the supernatants was determined using the Bradford assay (Bio-Rad protein assay; Bio-Rad Laboratories, Hercules, CA). One hundred fifty μ g of each lysate were mixed 1:4 with 4 \times SDS-PAGE loading buffer, boiled at 95°C for 5 minutes, and separated via 10% SDS-PAGE.

RNA Isolation

After dissection of the kidneys and other organs, the tissues were immediately frozen and ground in liquid

nitrogen. RNA was extracted using TRIzol reagent in accordance with the manufacturer's instructions and was further digested with DNase. Both reagents were purchased from Invitrogen Life Technologies, Carlsbad, CA. Cells were lysed directly in TRIzol reagent and processed as above. Integrity of RNA was determined by the appearance of distinct 28S and 18S rRNA bands when analyzed by electrophoresis on 1% agarose gels. The integrity of RNA was confirmed for all samples before microarray and reverse transcriptase (RT)-polymerase chain reaction (PCR) analysis.

Affymetrix Microarray Analysis

Gene expression profiling was performed by the Oregon Health and Science University Gene Microarray Shared Resource Affymetrix Microarray Core using MOE-430A chips, which contain 22,690 transcripts. Labeled target cDNA was prepared from purified total kidney RNA (10 μ g) from three saline- and three ricin-injected mice. The total RNAs were run on a 1% agarose gel and additionally analyzed on an Agilent Bioanalyzer to determine the integrity of 18S and 28S subunits of RNA. Each sample was hybridized to a test array and a MOE-430A GeneChip array. Image processing and normalization were performed using Affymetrix Microarray suite 5.0 (MAS 5.0) software to obtain the estimate of the fold change for each paired group (saline-injected mice and ricin-injected mice). Signals represent the abundance of each RNA transcript. A two-sample independent *t*-test was applied to each gene individually to identify differentially expressed genes and to estimate the average magnitude of differential expression. The resulting *P* values were adjusted using the false discovery rate proposed by Hochberg and Benjamini.³⁰ Genes with a false discovery rate *P* value of <0.05 and fold change of >3 or <-3 were selected as potentially significant genes. Genes with fold change <-3 belong to further studies.

Real-Time RT-PCR Analysis

Two μ g of RNA were reverse-transcribed in the presence of SuperScript II and oligo-dT primers (both reagents were purchased from Invitrogen Life Technologies). The amplification of the cDNA was accomplished using the ABI Prism 7900HT sequence detection system (Applied Biosystems, Foster City, CA) in the presence of the commercially available SYBR Green PCR Master Mix (Applied Biosystems) and 20 μ mol/L of the corresponding sense and anti-sense RT-PCR primers for 120-bp amplicons in a 40-cycle PCR (Table 1). Fold induction in gene expression was measured using absolute quantitation of a standard curve in arbitrary units. The denaturing, annealing, and extension conditions of each PCR cycle were 95°C for 15 seconds, 55°C for 30 seconds, and 72°C for 30 seconds, respectively.

Table 1. Forward and Reverse Primer Sequences Used for Real-Time RT-PCR

Gene	Forward primer sequence	Reverse primer sequence
TNF- α	5'-AAATGGGCTTTCCGAATTCA-3'	5'-CAGGGAAGAATCTGGAAAGGT-3'
IL-1 α	5'-AAAAAAGCCTCGTGCTGTCG-3'	5'-TTGTCGTTGCTTGGTTCTCCT-3'
IL-1 β	5'-CAAATCTCGCAGCAGCACA-3'	5'-TCATGTCCTCATCCTGGAAGG-3'
IL-6	5'-AGGATACCACTCCCAACAGACCT-3'	5'-CAAGTGCATCATCGTTGTTTCATAC-3'
GRO- α	5'-TGTCAGTGCCTGCAGACCAT-3'	5'-CGCGACCATTCTTGAGTGTG-3'
MCP-1	5'-AGCAGCAGGTGTCCCAAAGA-3'	5'-TCATTTGGTTCCGATCCAGG-3'
RANTES	5'-CCTGCTGCTTTGCCTACCTC-3'	5'-ACTTGGCGGTTCCCTCGAGT-3'
c-JUN	5'-GAAAACCTTGAAAGCGCAAAA-3'	5'-TAGCATGAGTTGGCACCCAC-3'
c-FOS	5'-TGGTGAAGACCGTGTCAGGA-3'	5'-GCAGCCATCTTATTCCGTTCC-3'
ATF3	5'-CGTCAACAACAGACCCCTGG-3'	5'-TTGTTTCGACACTTGGCAGC-3'
EGR-1	5'-CCTTCCAGTGTCCAATCTGCA-3'	5'-CTGGCAAACCTTCTCCACACA-3'
C/EBP β	5'-GGGACTTGATGCAATCCGG-3'	5'-AACCCCGCAGGAACATCTTT-3'
E-selectin	5'-ACTGTGTGCAAGTTCGCCTG-3'	5'-TGGACTCAGTGGGAGCTTCAC-3'
GAPDH	5'-TTGTGGAAGGGCTCATGACC-3'	5'-GATGCAGGGATGATGTTCTGG-3'

Sense and Anti-Sense RT-PCR Primer Sequences

All murine forward and reverse primers (Table 1) were designed by using MacVector or Primer Express software programs and were synthesized by Invitrogen Life Technologies.

Reverse Transcription of rRNA by Primer Extension

Reverse transcription of rRNA was performed as described by Iordanov and colleagues.⁵ The oligonucleotide primer 5'-CACATACACCAAATGTC-3' (Invitrogen Life Technologies) was end-labeled with T4 polynucleotide kinase (Life Technologies, Inc.). A 10- μ l mixture of 2 μ g total RNA and 1.0 pmol primer in 50 mmol/L Tris-HCl (pH 8.3), 75 mmol/L KCl, 3 mmol/L MgCl₂ was incubated at 90°C for 3 minutes and then placed on ice for 5 minutes, followed by an incubation at room temperature for 5 minutes. The reverse transcription was initiated by the addition of 10 μ l of a mixture of 2 mmol/L deoxynucleoside triphosphates and 30 U SuperScript (Life Technologies, Inc.) in 50 mmol/L Tris-HCl (pH 8.3), 75 mmol/L KCl, 3 mmol/L MgCl₂, 10 mmol/L dithiothreitol, followed by an incubation at 48°C for 15 minutes, when the reactions were stopped by the addition of 5 mmol/L EDTA. Reaction products were precipitated in ethanol, resuspended in formamide gel loading buffer, heat denatured, and electrophoresed in 8% acrylamide sequencing gel, which was subsequently dried and exposed to a PhosphorImager screen.

Immunohistochemical Analysis

For detection of phospho-p38 MAPK, phospho-ERK1/2, and phospho-JNK, mice were anesthetized (see above) and perfused through the heart with 10 ml of 0.9% NaCl (LabChem Inc., Pittsburgh, PA) to flush the circulation, followed by 30 ml of 4% paraformaldehyde. After dissection, the organs were further fixed in 4% paraformaldehyde solution for 48 hours, processed in an automatic tissue processor, embedded in paraffin blocks, and sec-

tioned into 7- μ m sections. Before immunohistochemical staining, the tissue sections underwent antigen-retrieval procedures in accordance with the instructions provided with the corresponding primary antibody. For detection of fibrin(ogen), mice were sacrificed by cervical dislocation. The organs were dissected, fixed in Carnoy solution for 2 hours, transferred to 70% ethanol, and further processed in an automatic tissue processor as described above. The tissue sections were incubated for 24 hours with goat polyclonal antibody against mouse fibrin(ogen).

Mouse Blood Studies

All blood analyses were performed by the Core Laboratory, Division of Laboratory Medicine, Oregon Health and Science University, Portland, OR. Blood was obtained by a puncture of the retro-orbital plexus. Blood for cell-count analysis and cell-type determination was collected in hematology tubes with tripotassium ethylenediaminetetraacetic acid (EDTA) (Microtainer; Becton Dickinson, Franklin Lakes, NJ) and analyzed with an automated cell counter (Beckman-Coulter, Inc., Fullerton, CA). Biochemical determinations of blood urea nitrogen and serum creatinine were performed with a Synchron LX Clinical Chemistry System (Diagnostic Chemicals Ltd., Oxford, CT).

Gel Electrophoresis of Hemoglobin

Total blood, obtained by puncture of the retro-orbital plexus, was left to clot at room temperature for 1 hour, and was then centrifuged at 8000 rpm, 4°C, for 20 minutes to separate serum from blood cells. Ten μ l of serum were mixed 1:1 with 2 \times sample buffer (20% glycerol, 150 mmol/L Tris-HCl, pH 9.2, bromophenol blue) and run on 1.5% agarose gels in the presence of Tris-glycine electrophoresis buffer (130 mmol/L Tris, 95 mmol/L glycine, pH 9.2). Gels were stained with Gelcode Blue staining solution (Pierce, Rockford, IL). Hemoglobin, isolated from lysed erythrocytes in 0.065 mol/L KCl, was used as positive control.

Proteinuria Studies

Mice were housed in diuresis metabolic cages for 24 hours during which time urine was collected. Urine was further concentrated through 30-kD Micropore concentration tubes. Equal amounts of urine from three control mice and three ricin-injected animals were mixed 1:4 with 4× SDS-PAGE loading buffer, boiled at 95°C for 5 minutes, and separated via 10% SDS-PAGE. Gels were stained with Gelcode Blue staining solution. Increasing concentrations of bovine serum albumin were loaded on the same gel as a positive control.

Statistical Analysis

Individual groups were compared using unpaired *t*-test analysis. To estimate *P* values, all statistical analyses were interpreted in a two-tailed manner. *P* values <0.05 were considered to be statistically significant.

Results

Ricin and the Inflammatory Cascade in RAW 264.7 Macrophages

To examine the ability of ricin to induce inflammatory responses *in vitro*, we used RAW 264.7 cells, a murine monocyte/macrophage cell line that has been used frequently to examine responses to proinflammatory agents.^{31,32} Concentrations of ricin as low as 10 ng/ml induced the phosphorylation of JNK, p38 MAPK, and ERK1/2 (Figure 1a). A direct relationship was observed between the phosphorylation of these kinases and the inhibition of protein translation (Figure 1b); 10 ng/ml of ricin reduced the incorporation of [³H]-leucine into protein by ~50%, whereas higher doses inhibited the level of leucine incorporation by 97%.

The administration of ricin to cultured cells leads to increased transcription and translation of several inflammatory mediators, including TNF- α , IL-1 β , and chemokines.^{33–35} In view of the well-described role of p38 MAPK in regulating the expression of TNF- α ,^{11,36,37} we applied quantitative real-time RT-PCR to examine the influence of ricin on the abundance of mRNAs that encode TNF- α . Throughout the evaluated range of concentrations, ricin induced a 12-fold increase in the abundance of RNA encoding TNF- α (Figure 1c). Exposure of cells to 10 and 100 ng/ml of ricin led to a 10-fold increase in the secretion of TNF- α protein into the medium of treated cells, whereas higher concentrations of the toxin were less effective in elevating the release of TNF- α (Figure 1d). Taken together, these data reveal a strong positive correlation between the activation of all three MAPK members (JNKs, p38 MAPK, and ERK1/2), the increased expression of TNF- α RNA, and the increased secretion of TNF- α protein in ricin-treated cells. These data further indicate that, despite the substantial but incomplete inhibition of protein translation at intermediate concentrations of ricin (10 and 100 ng/ml), cells exposed to ricin nevertheless retained the ability to translate TNF- α

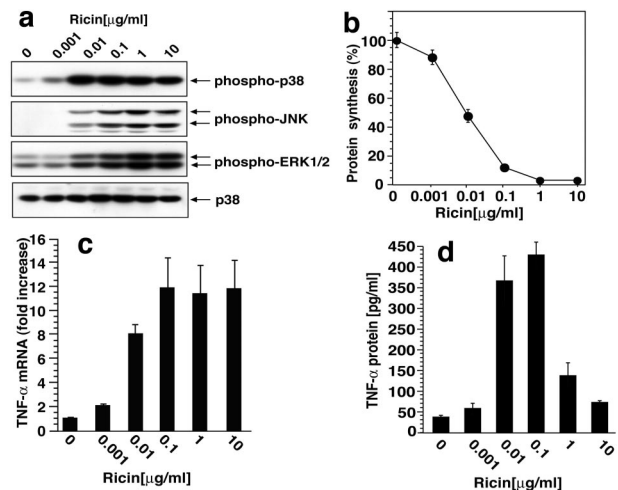


Figure 1. Response of RAW 264.7 cells to ricin. **a:** Immunoblot analysis of cell lysates after exposure to varying doses of ricin. Antibodies used were reactive against phospho-ERK1/2, phospho-p38 MAPK, phospho-JNK, and p38 MAPK, as shown. Cells were harvested 4 hours after the addition of ricin. **b:** Inhibition of protein synthesis measured by [³H] leucine incorporation 3 hours after the addition of varying concentrations of ricin. Each treatment was performed in triplicates. Data are presented as means ± SEM. **c:** TNF- α mRNA abundance measured by real-time RT-PCR, 5 hours after exposure to varying concentrations of ricin. Representative data from three different experiments are shown. Each treatment was performed in triplicates. Data are presented as means ± SEM. **d:** Ricin-induced release of TNF- α protein into the culture medium was measured by ELISA; media were harvested 6 hours after the addition of ricin. Representative data from three different experiments are shown. Each treatment was performed in triplicates. Data are presented as means ± SEM.

mRNA and to secrete TNF- α into the medium. The inability of cells to secrete TNF- α after exposure to high concentrations of ricin (1 and 10 µg/ml) may stem from the nearly complete abrogation of protein translation at these concentrations. Despite the inhibition of protein synthesis induced by intermediate concentrations of ricin, the concomitant increase in mRNA encoding TNF- α may thus serve to overcome the cell's impaired capacity to translate and secrete TNF- α protein.

JNK, p38 MAPK, and ERK1/2 regulate the expression of mRNAs that encode inflammatory cytokines and chemokines in part by increasing the expression of specific transcription factors.^{11,38,39} We determined the potential contribution of these three MAPK family members in regulating the ricin-induced expression of mRNAs encoding selected cytokines and transcription factors by selectively blocking their activation and measuring the abundance of RNA by real-time RT-PCR. To accomplish this, we applied highly specific inhibitors, singly and in combination, that are known to interfere with effective transduction of JNK, p38 MAPK, and ERK1/2 cascades (SP600125 for JNK, SB203580 for p38 MAPK, and UO126 for ERK1/2). We confirmed the effectiveness and specificity of these inhibitors in RAW 264.7 cells by applying immunoblotting with phospho-specific antibodies against these kinases and/or their downstream-phosphorylated targets (data not shown). Five hours after the addition of ricin, the abundance of mRNAs that encode TNF- α , IL-1 α , and IL-1 β were elevated several fold. The increase in ricin-induced expression of TNF- α mRNA was reduced partially by each of the kinase inhibitors when

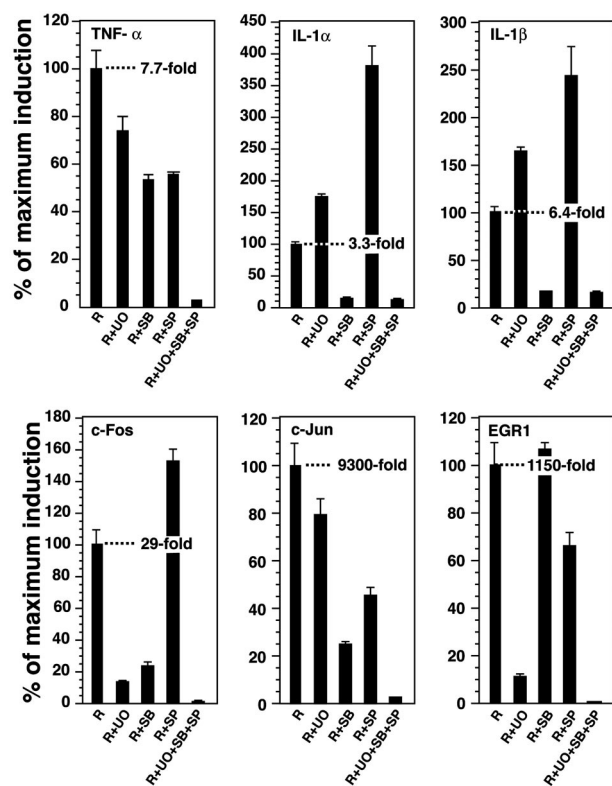


Figure 2. Real-time RT-PCR analysis of RNA in RAW 264.7 cells 5 hours after the addition of 1 μ g/ml of ricin. Cells were pretreated for 30 minutes with selective inhibitors of the MAPK family members [20 μ mol/L SP600125 (SP) for JNK, 10 μ mol/L SB203580 (SB) for p38 MAPK, and 10 μ mol/L UO126 (UO) for ERK1/2] or with DMSO as a vehicle control. Ricin (R) was then added (0.1 μ g/ml) for 5 hours, at which time RNA was isolated. GAPDH was used as a comparator to obtained fold induction, whose value is shown in each panel. Data are expressed as percentage of maximal induction to permit relative comparisons among the six genes whose expression was analyzed. Each treatment was performed in triplicates; error bars represent SEM.

applied separately; in the presence of all three inhibitors, the expression of TNF- α was suppressed to near basal levels (Figure 2). In contrast, the increased expression of RNAs that encode IL-1 α and IL-1 β was completely suppressed by the inhibition of p38 MAPK alone; the inhibition of JNK or ERK1/2 led to an increase in the expression of IL-1 mRNA.

The genes of many inflammatory mediators are known to contain regulatory sites that bind AP-1 transcription factors, a family of dimeric basic leucine zipper DNA-binding proteins that include c-Fos, c-Jun, and ATF-4.⁴⁰ Many of the AP-1 factors are ultimate targets that lie downstream of p38 MAPK, JNK, and ERK signaling pathways. As we have previously demonstrated, the exposure of cultured cells to ricin leads to a sustained increase in the levels of mRNAs that encode c-Fos and c-Jun.⁵ The 30-fold increase in the ricin-induced expression of c-Fos mRNA was reduced substantially by inhibiting p38 MAPK or ERK1/2 but not by inhibiting JNK (Figure 2). The combined inhibition of both p38 MAPK and ERK1/2 suppressed the ricin-induced expression of c-Fos mRNA to basal levels (data not shown) that were indistinguishable from the levels achieved in the presence of all three inhibitors. Administration of ricin elevated the expression of c-Jun mRNA more than 9000-fold; this increase was

partially reduced by each of the inhibitors and reduced to less than 3% of maximally induced values by the combination of all three inhibitors (Figure 2).

EGR-1 is a transcription factor and immediate-early gene product that induces the expression of TNF- α via activation of the MAPK cascade.^{41–43} Ricin induced the expression of EGR-1 RNA more than 1000-fold; this increase was partially suppressed by inhibiting JNK and ERK1/2 individually, but not by inhibiting p38 MAPK (Figure 2). The inhibition of both JNK and ERK1/2 pathways completely reduced the activation of EGR-1 by ricin (data not shown). Taken together, the results shown in Figure 2 suggest that the activation by ricin of JNK, p38 MAPK, and ERK1/2 regulates the expression of RNAs encoding a variety of inflammatory cytokines and the transcription factors that are known to contribute to their activation. These data further suggest that some genes receive activating signals from multiple MAPKs, whereas other genes receive activating signals through a single predominant MAPK pathway. The data in Figures 1 and 2 support the hypothesis that ricin-induced activation of MAPK members is necessary for the expression of genes that encode inflammatory mediators and transcription factors that have been associated with their expression. The increased accumulation of some RNAs after the selective inhibition of a single MAPK pathway suggests that certain MAPK members may act to suppress the expression of some genes.

An Animal Model of Ricin Intoxication

Taylor and colleagues¹³ used ricin to reproduce a model of toxin-induced HUS in rats that recapitulated many of the hallmarks of the human disease including thrombocytopenia, hemolytic anemia, renal failure, and microvascular thrombosis. We applied a similar approach in mice to be able to exploit the power of mouse genetics to examine the mechanisms and consequences of ricin intoxication in a mouse model. We injected 12 μ g per 100 g body weight ricin intravenously, through the retro-orbital venous plexus, into groups of mice, and sacrificed the animals 24 hours after the administration of the toxin. Ricin-injected mice displayed thrombocytopenia that was marked by a 75% decrease in the number of thrombocytes (Figure 3C). The number of erythrocytes was diminished by 50% and the hemoglobin concentration decreased to 40% of control values (Figure 3, A and B). The decrease in erythrocyte numbers and hemoglobin concentration in ricin-treated mice are consistent with the development of anemia, which was further determined to be normocytic (normal values of the mean corpuscular volume; data not shown), normochromic (normal values of the mean corpuscular hemoglobin concentration; data not shown), and regenerative (increased count of the reticulocytes in the peripheral blood; data not shown). The appearance of free hemoglobin in the sera of ricin-treated mice (Figure 3, I and J) provided evidence for intravascular hemolysis. Interestingly, microscopic examination of blood smears did not reveal unequivocal evidence for the appearance of schistocytes (data not

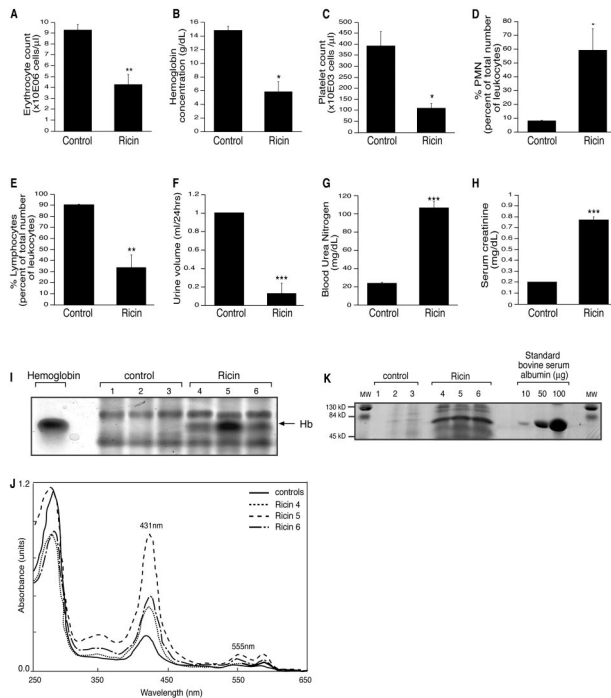


Figure 3. Analysis of blood and urine after administration of ricin *in vivo*. **A–E, G–H:** Analyses of blood from three sham-injected mice and six mice injected with 12 μ g of ricin/100 g body weight. Data are presented as mean \pm SEM; *, $P < 0.05$; **, $P < 0.01$; and ***, $P < 0.001$. **A, B:** Development of anemia after intravenous ricin administration, determined by a decrease in the erythrocyte count and hemoglobin concentration. **C:** Thrombocytopenia. **D, E:** Increased numbers of polymorphonuclear leukocytes and decreased number of lymphocytes. **G, H:** Evidence of renal failure, as determined by increased concentrations of serum creatinine (**G**) and blood urea nitrogen (**H**). **F:** Decreased urine volume in mice that received 12 μ g of ricin/100 g body weight compared to the saline-injected controls. Error bars show SEM; ***, $P < 0.001$. **I:** Appearance of free hemoglobin in the serum of mice that received ricin. Equal amounts of serum from three saline (1, 2, and 3) and three mice injected with 12 μ g of ricin/100 g body weight (4, 5, and 6) were separated by charge by electrophoresis under nondenaturing conditions. Hemoglobin (Hb) isolated after 0.065 mol/L KCl lysis of erythrocytes was used as a positive control. **J:** The appearance of free hemoglobin in all of the animals that received ricin. **K:** Absorption spectrophotometry of sera from **I** demonstrates absorbance maxima at 431 nm and 555 nm, characteristic of hemoglobin. An increase in the absorbance peaks at these maxima was observed in the sera of mice injected with ricin. Although the peaks of hemoglobin absorbance maxima were lower for each of the control mice, the control sera were pooled in this figure to facilitate graphic representation. **L:** Albuminuria after ricin administration. Equal amounts of urine from three saline-injected mice (1, 2, and 3) and three mice injected with 12 μ g of ricin/100 g body weight (4, 5, and 6) were run on a 10% SDS-PAGE. Representative data are shown from two different experiments, each treatment performed in triplicate. Bovine serum albumin at increasing concentrations (10, 50, and 100 μ g) was used as a standard. MW stands for molecular weight of the commercially available protein markers.

shown). Mice that received ricin displayed an eightfold increase in the number of circulating polymorphonuclear leukocytes accompanied by a 30% decrease in the number of lymphocytes (Figure 3, D and E).

An important hallmark of human HUS is the development of renal failure. Mice treated with ricin showed a decrease in the 24-hour urinary output compared with control mice (Figure 3F). To further investigate the effects of ricin on kidney function, we evaluated the serum levels of blood urea nitrogen and creatinine. The serum levels of blood urea nitrogen and creatinine in mice that received ricin were elevated approximately fourfold (Figure 3, G and H). Taken together, the decreased urinary output, the

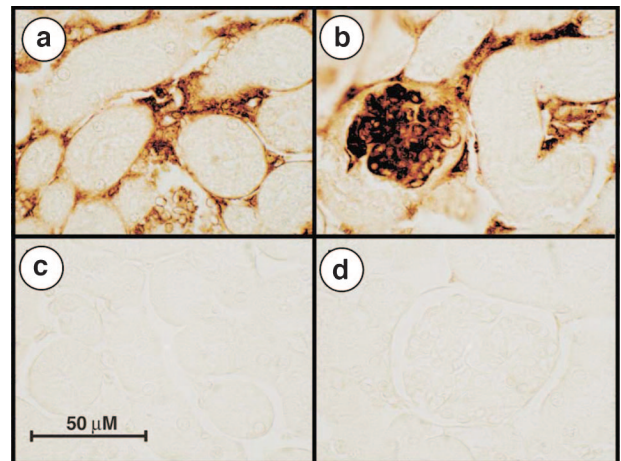


Figure 4. Immunohistochemical localization of fibrin(ogen) in kidneys of ricin-treated animals. Mice injected with saline (**c, d**) or 12 μ g/100 g body weight ricin (**a, b**) were sacrificed 24 hours after the injections. Carnoy-fixed tissues were embedded in paraffin and sections were reacted with primary goat polyclonal antibody against mouse fibrin(ogen). Kidneys of ricin-injected mice display fibrin(ogen) depositions in the glomerular capillary loops (**b**) and in the peritubular microvasculature (**a**). Representative pictures from two independent experiments, each performed in triplicate animals, are shown.

increased serum concentrations of blood urea nitrogen and creatinine provided evidence that administration of ricin resulted in compromised renal function. Additionally, the urine obtained from ricin-treated mice displayed an increased excretion of protein; the major protein band corresponded in size to serum albumin (Figure 3K).

Histopathological examination of hematoxylin and eosin (H&E) staining of tissue after administration of ricin showed evidence of massive apoptosis (by the appearance of nuclear fragmentation and apoptotic bodies) in the red pulp and some in the white pulp of the spleen, patchy apoptosis of hepatocytes ranging from periportal to panlobular localization, apoptotic debris in the glomeruli, and randomly dispersed single apoptotic tubular epithelial cells. After H&E staining, there was no evidence of glomerular thrombosis or tubular epithelial cell necrosis.

To investigate the appearance of thrombotic microangiopathy, a distinguishing feature of human HUS,⁴⁴ we used immunohistochemical staining with an anti-fibrin(ogen) antibody. The staining revealed the appearance of abundant deposition of fibrin(ogen) in the glomerular capillary loops as well as in the peritubular microvasculature of ricin-treated mice (Figure 4). We observed a similar localization of fibrin(ogen) in the microvasculature of liver and lungs in ricin-treated mice (not shown).

Ricin Induces the Activation of ERK, p38, and JNK in Kidneys and Other Organs of Ricin-Treated Mice

Because the kidneys appeared to constitute a relevant and potentially important target for the actions of ricin, we concentrated our studies on this organ. In view of the demonstration that exposure of cultured murine macrophages to ricin resulted in activation of JNK, p38 MAPK, and ERK1/2 (Figure 1a), we tested the ability of intrave-

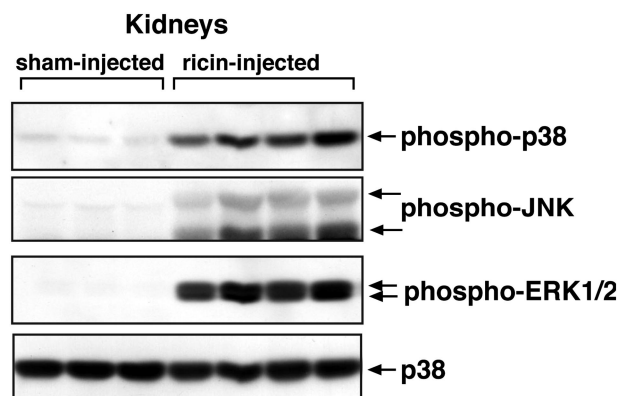


Figure 5. Activation of p38 MAPK, JNK, and ERK1/2 in kidneys of mice injected with ricin. Kidney lysates from three sham-injected mice and four mice injected with 12 μ g of ricin/100 g body weight were analyzed by immunoblotting with antibodies against phospho-ERK1/2, phospho-p38 MAPK, and phospho-JNK. Results demonstrate activation of all three MAPK family members after ricin administration. Immunoblotting with anti-p38 MAPK antibody was used as a loading control. This experiment was performed three times; each treatment group included six animals. Representative data from one experiment is shown, each sample representing kidney lysate from an individual animal.

nously administered ricin to activate these kinases in the kidneys of mice. Twenty-four hours after the injection of ricin, the phosphorylation of ERK1/2, p38 MAPK, and JNK increased dramatically in the kidneys (Figure 5) and in other organs of mice such as lung, spleen, and heart (data not shown). Increased phosphorylation of these kinases was also detected by immunohistochemical localization in tissue sections of kidneys from ricin-treated mice that had been perfused with paraformaldehyde. When compared to the sham-injected counterparts, glomerular and peritubular microvascular cells of ricin-treated mice displayed a marked increase in the phosphorylated forms of ERK1/2, p38 MAPK, and JNK (Figure 6). In addition, ricin induced increased reactivity of all of the three kinases in the nuclei of some proximal and distal convoluted tubules in the periglomerular region. Examination of several other organs (heart, liver, spleen, lungs) revealed similar expression of the phosphorylated forms of the MAPKs in endothelial cells and other cell types, including cardiac myocytes, hepatocytes, and splenic lymphocytes (data not shown).

Affymetrix Microarray Analysis

The prominent nuclear localization of activated MAP kinases (Figure 6) suggests that activated MAPK members participate in the transcriptional activation of genes in organs of ricin-injected mice. To identify genes activated in kidneys of ricin-treated mice, we performed Affymetrix microarray analyses on kidneys of three sham-injected and three ricin-injected animals 24 hours after the intravenous administration of 12 μ g per 100 g body weight of toxin. Analyses were performed on MOE-430A chips, which interrogate 22,690 mouse transcripts. Genes that were consistently absent from all six samples were excluded from the analysis, reducing the number of evaluated genes to 17,718. Of the annotated genes (genes of known or suspected function), 918 were declared up-

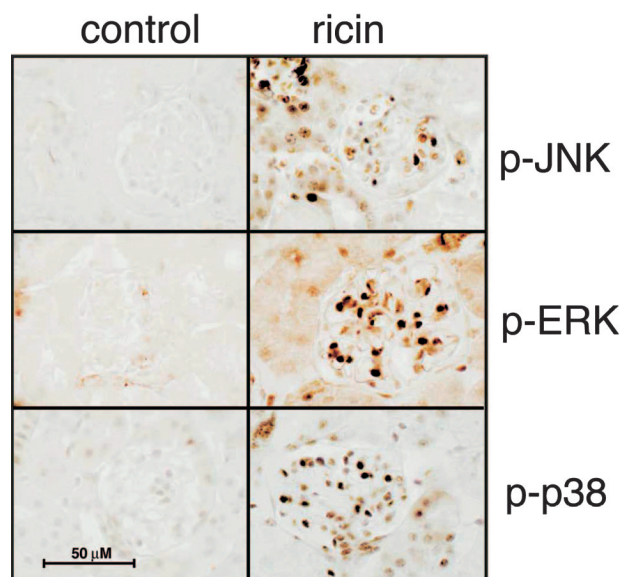


Figure 6. Ricin induces the phosphorylation of ERK, JNK, and p38 MAPK in glomerular cells. Immunohistochemical staining with phospho-ERK1/2, phospho-p38 MAPK, and phospho-JNK antibodies performed on kidney tissue sections of control and ricin-injected mice (12 μ g/100 g body weight i.v. for 24 hours.) after fixation by perfusion with 4% paraformaldehyde solution. Each image contains one representative glomerulus. Immunohistochemical staining reactions were performed on sections from animals from three different experiments, each performed on groups of six mice.

regulated after ricin administration (fold change >3 and a false discovery rate adjusted P value <0.05). Of these, 46 annotated genes were identified in the Affymetrix array as displaying a level of induction of 20-fold or greater. The microarray analysis (Appendix Table 1) in Excel format is accessible at <http://ajp.amjpathol.org>.

The data from the microarrays were analyzed by EASE, a software application for the rapid interpretation of biological data obtained from microarray analysis.⁴⁵ The EASE software automates the process of biological theme determination by analyzing the overrepresentation of genes that belong to categories that are functionally and structurally defined. Table 2 displays the hierarchical analysis of the 46 annotated genes whose expression was induced greater than 20-fold in this experiment. These data reveal that the most highly overrepresented genes activated after injection of ricin were associated with inflammatory responses and wounding. The molecular functions of these induced genes were identified as cytokines, chemokines, and transcription regulators.

Table 3 displays a subset of genes, identified in the microarrays, whose transcripts were elevated by ricin and whose functions have been associated with inflammatory responses and activation by stressors. Many of the induced mRNAs that encode transcriptional regulators such as c-Jun,⁴⁶ c-Fos,⁴⁶ ATF3,^{47–49} and C/EBP β ^{50,51} have appeared in previous studies as immediate-early genes whose expression has been tied to ligands that activate ERK, p38 MAPK, and JNK. Several of these transcriptional regulators have been shown to bind to regulatory sequences of genes encoding cytokines and chemokines. The coordinately increased expression of transcriptional regulators and cytokines/che-

Table 2. Overrepresentation Analysis of Annotated Ricin-Induced Gene Expression

	Hits	Total in category	P value (EASE score)
Biological process			
Inflammatory response	7	103	7.85e-006
Response to wounding	7	145	5.50e-005
Cell proliferation	7	145	6.39e-005
Regulation of cell cycle	8	276	2.75e-004
Response to stress	10	477	3.16e-004
Regulation of transcription	16	1255	4.00e-004
Immune response	9	415	6.19e-004
Receptor binding	8	406	2.19e-003
Defense response	9	527	2.86e-003
Molecular function			
Cytokine activity	8	185	1.78e-005
Chemokine activity	5	36	1.98e-005
Transcription regulator activity	14	934	1.80e-004
Receptor binding	8	406	2.19e-003
DNA binding	15	1481	4.66e-003
Protein binding	14	1442	9.89e-003

mokines is consistent with the hypothesis that the increased expression of transcription factors is positioned upstream of, and is directly responsible for, the increased expression of cytokines and chemokines.

In addition to the genes noted above, the administration of ricin led to the increased expression of RNAs encoded by other genes of interest, such as those involved in leukocyte adhesion (ICAM-1,⁵² P-selectin,⁵³ E-selectin⁵³) or those that participate in MAPK signaling pathways (Cnk,⁵⁴ MAP3k8,⁵⁵ and MAPk6⁵⁶). The microarrays also revealed elevated ricin-induced expression of genes that belong to several members of the coagulation cascade and fibrinolytic pathway such as factor I (fibrinogen), factor III (tissue factor), factor X (prothrombinase), u-PA receptor, and PAI-1.

Real-Time RT-PCR Analysis of Ricin-Induced RNAs in Kidneys

Although Affymetrix microarray analysis aids in identifying genes that are coordinately regulated after ricin administration, the ability of the microarrays to provide accurate quantitative data are limited. To provide a more rigorous quantitative analysis of ricin-induced gene expression, and to validate the results from microarray analysis, we applied real-time RT-PCR to measure the expression in mouse kidney of several RNAs that encode proteins implicated in inflammatory responses. Groups of three sham-injected and three ricin-injected mice were sacrificed at varying times, after which RNA was extracted from the kidneys for analysis by real-time RT-PCR. The gene products evaluated included cytokines (TNF- α , IL-1 α , IL-1 β , and IL-6), chemokines [MCP-1 (CXCL1) and Gro- α (CCL2)], transcription factors (c-Jun, c-Fos, ATF3, C/EBP β , and EGR1), and E-selectin. The results were expressed as fold induction, using glyceraldehyde phosphate dehydrogenase (GAPDH) as an invariant comparator.

The administration of ricin significantly elevated the expression of each of the mRNAs that were investigated (Figure 7). The ricin-induced expression of most genes

began at 6 hours and continued to increase until the termination of the experiment (18 hours). The expression profile of mRNA encoding IL-1 α and IL-1 β showed an early peak at 6 hours followed by a decline at 10 hours and a second peak of expression thereafter. The expression of E-selectin RNA deviated from the expression profiles of the other examined genes inasmuch as the peak of expression occurred at 10 hours and declined thereafter.

Ribotoxic Damage to A4256 in the Mouse Kidney

Ricin may impair kidney function by acting directly on cells of the kidney or by inducing the release of inflammatory mediators into the systemic circulation from cells or tissues that lie outside the kidney. To determine whether ricin acts directly on the kidney, we applied primer-extension analysis to identify the depurination of 28S rRNA by ricin. Figure 8a shows a primer-extension analysis of RNA extracted from control or ricin-treated human macrophages (THP-1) *in vitro* (lanes 1 and 2) and kidneys from mice that were either untreated (lane 3) or injected with ricin (lane 4). When examined by primer-extension analysis, RNA extracted from THP-1 cells and kidneys exposed to ricin displayed a strong stop in extension of the complementary DNA transcript at the expected adenine (circled). To quantify the percentage of lesions present in extracted RNA, we included dideoxy-GTP in the transcription mixture to yield strong stops at guanines (complementary to the cytosines in the figure). The RNA from ricin-treated cells revealed less radioactivity in the guanosine-specific bands situated above (on the 5' site of) the lesions at A4324 when compared with RNA from control cells (lane 1). By using analytical software (IP LabGel) to measure the decrease in intensity of the guanines 5' to the lesion, when compared with the intensity of guanines 3' to the lesion, we determined that ~80% of the 28S rRNA from THP-1 cells contained lesions at A4565. Using the same calculations, we determined that ~30% of the 28S rRNA of ricin-treated kidneys

Table 3. Ricin-Induced Transcripts Compiled from Affymetrix Microarrays

Gene	Accession number	Fold induction	P value	Function of gene product
Transcription regulators				
MafF	BC022952.1	741	<0.001	b-Zip transcriptional activator
Egr2	X06746.1	245	<0.01	Zinc finger transcriptional activator
ATF3	BC019946.1	188	<0.01	Stress-induced immediate-early gene
RelB	NM009946.1	76	<0.001	NF- κ B family, induced by TNF, IL-1, IL-6
c-Fos	AV026617	74	<0.001	Stress-induced immediate-early gene
c-Myc	BC006728.1	58	<0.001	Involved in activation of genes in G ₁
Egr1	NM007913.1	49	<0.001	Mitogen-induced zinc finger protein
c-Jun	BC002081.1	40	<0.001	AP-1 member, regulator of TNF and IL-1
C/EBP β	NM009883	36	<0.001	CAAT-binding protein
JunB	NM008416.1	26	<0.001	AP-1 member
ATF4	AV314773	13	<0.001	Transcription factor
Egr4	NM020596.1	12	<0.01	Zinc finger transcriptional activator
STAT2	BB030134	11	<0.001	Transcriptional activator and signal transducer
FosB	NM0080036.1	8	<0.001	AP-1 member
MafK	NM010747.1	8	<0.001	Transcriptional regulator
RelA	NM009045.1	7	<0.001	Transcriptional activator
Chemokines and cytokines				
CXCL2	NM009140.1	110	<0.001	Gro- β ; CXC chemokine
CXCL1	NM008176.1	98	<0.001	Gro- α ; CXC chemokine
IL-6	NM031168.1	75	<0.001	Inflammatory cytokine
CXCL10	NM021274.1	63	<0.001	IP-10; CXC chemokine
CXCL9	NM008599.1	37	<0.001	Mig; CXC chemokine
CCL2	AF065933.1	36	<0.001	MCP-1; CC chemokine
M-CSF	M21149.1	36	<0.01	Macrophage-stimulating factor
IL-1 β	BC011437.1	6	<0.01	Inflammatory cytokine
Leukocyte adhesion molecules				
P-selectin	M72332.1	23	<0.001	Leukocyte adhesion protein
ICAM-1	BC008626.1	22	<0.001	Leukocyte adhesion protein
Syndecan-1	BI788645.1	16	<0.01	Endothelial-leukocyte interactions
E-selectin	NM011345.1	4	<0.01	Leukocyte adhesion protein
Growth factors				
Amphiregulin	NM009704.1	43	<0.001	EGF family growth factor
Gdf15	NM011819	40	<0.001	TGF- β family; induced by organ injury
PDGF-B	BC023427.1	7	<0.01	Platelet-derived growth factor
Kinases				
Cnk	BM947855	330	<0.001	Cytokine-inducible serine/threonine kinase
Map3k8	NM007746.1	39	<0.001	Stimulates JNK and p38 MAPK in stress
MAPK6	NM015806.1	22	<0.001	MAPK family member
Coagulation cascade and fibrinolysis				
PAI-1	NM00887.1	31	<0.001	Physiological inhibitor of tissue plasminogen activator
Factor III	BC024886.1	7	<0.001	Co-factor w/ factor VIIIa to activate factor X in extrinsic pathway of coagulation
UPAR	X62701.1	6	<0.001	Urokinase plasminogen activator receptor
Factor X	NM008013.1	5	<0.001	Prothrombinase/fibrinogen-like protein 2
Fibrinogen, α peptide	BC005467.1	4	<0.001	Yields monomers that polymerize into fibrin; co-factor in thrombocyte aggregation

(lanes 3 and 4) contained lesions. The number of lesions that appeared in 28S rRNA of kidneys increased directly with time after administration of ricin (Figure 8b), indicating that the intracellular lesions resulting from ricin toxicity continued to accumulate.

Gene Expression in Mouse Kidney after Co-Administration of Ricin and LPS

It has been suggested that LPS/endotoxin has been involved together with Stx in the pathogenesis of HUS.^{15,57,58} Several *in vivo* and *in vitro* studies report cooperation between Stx and LPS in producing pathological changes similar to those observed in the human HUS.^{59–61} To determine the effect of LPS on gene acti-

vation in the presence or absence of ricin, we injected mice with LPS, ricin, or LPS plus ricin and by real-time RT-PCR measured the induction of mRNA that encode several proteins associated with the inflammatory response (Figure 9). Injection of LPS alone minimally affected the abundance of all mRNAs except the chemokine RANTES (CCL5). The combination of LPS plus ricin significantly elevated RNAs that encode TNF- α , IL-6, MCP-1 (CCL2), RANTES (CCL5), GRO- α (CXCL1), and E-selectin over levels observed after injection of ricin alone. In contrast, compared with ricin alone, LPS plus ricin failed to significantly increase the RNAs that encode IL-1 α , IL-1 β , or the transcription factors EGR-1, C/EBP β , and ATF-3. These data suggest that, at the concentration of LPS injected, LPS alone was unable to drive the ex-

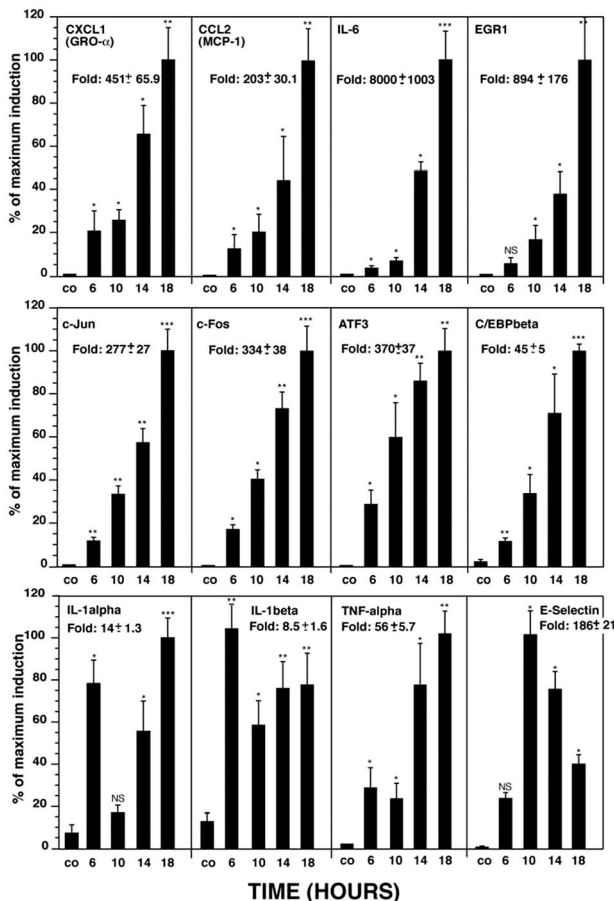


Figure 7. Real-time RT-PCR analysis of ricin-induced gene expression in mouse kidney. Groups of three mice received intravenously 12 μ g of ricin/100 g body weight and were sacrificed at the designated times when kidneys were removed. After RNA extraction, real-time RT-PCR analysis was performed using primers to the corresponding genes. Error bars represent SEM. *P* values are as follows: *, *P* < 0.05; **, *P* < 0.01; ***, *P* < 0.001; and NS, nonsignificant.

pression of most of the inflammatory genes that were examined. These results suggest that the signaling pathways stimulated by LPS may synergize with, or complement, those stimulated by ricin for the activation of these genes.

Expression of TNF- α , IL-1 β , and IL-6 Protein in the Serum of Ricin-Treated Mice

We assessed whether the administration of ricin to animals would lead to an elevation of the serum levels of protein encoded by the cytokines whose mRNA expression was induced by ricin. Groups of three sham-injected and ricin-injected mice were exsanguinated 24 hours after administration, and the serum levels of TNF- α , IL-1 β , and IL-6 were analyzed by ELISA. The levels of TNF- α increased from 16 ± 1.7 to 92 ± 30 pg/ml (*P* < 0.05) 24 hours after ricin injection. The levels of IL-1 β increased from 0.33 ± 0.01 ng/ml to 0.68 ± 0.13 ng/ml (*P* < 0.05) in ricin-treated animals and levels of IL-6 increased from 1.8 ± 0.2 to 13 ± 1.1 ng/ml (*P* < 0.01). These data suggest that the ricin-induced increase in the expression

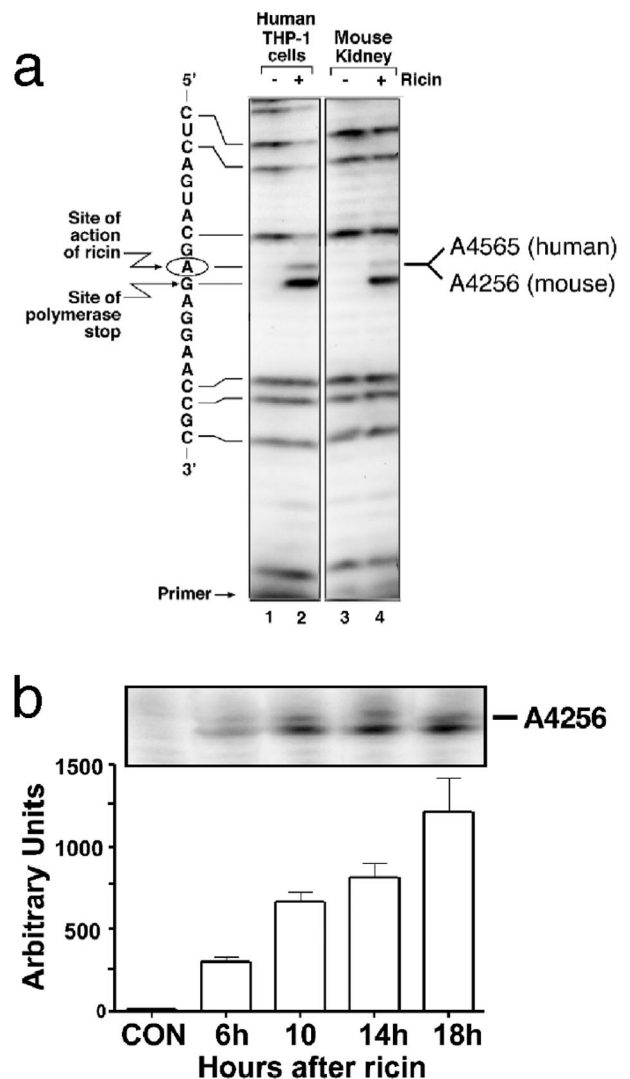


Figure 8. Primer-extension analysis of ricin-induced lesions in 28S rRNA in mouse kidney. **a:** THP-1 cells were exposed to vehicle alone (lane 1) or 1 μ g/ml of ricin for 6 hours (lane 2); kidneys from either sham-injected (lane 3) or ricin-injected (12 μ g of ricin/100 g body weight; lane 4) mice were harvested 24 hours after the injection. The circled adenine indicates the site of action of ricin within the sarcin/ricin loop of 28S rRNA. **b:** Ribotoxic damage of A 4256 in 28S rRNA from kidneys after ricin administration *in vivo*. Animals were injected with saline (CON) or ricin (12 μ g/100 g body weight) and were sacrificed at the times shown. Error bars represent SEM.

of RNA encoding TNF- α , IL-1 β , and IL-6 was associated with a significant increase in the serum levels of those cytokines. Importantly, these data demonstrated that the induced expression of mRNA associated with ricin intoxication may result in the increased synthesis of proteins directed by those RNAs, even in the face of potentially decreased levels of protein synthesis.

Discussion

Our earlier studies have demonstrated that depurination of 28S rRNA by ricin results not only in the inhibition of protein translation, but also in the intense and extended activation of the SAPKs.⁵⁻⁹ Of the SAPKs, p38 MAPK is known to be a central signal transducer of inflammatory

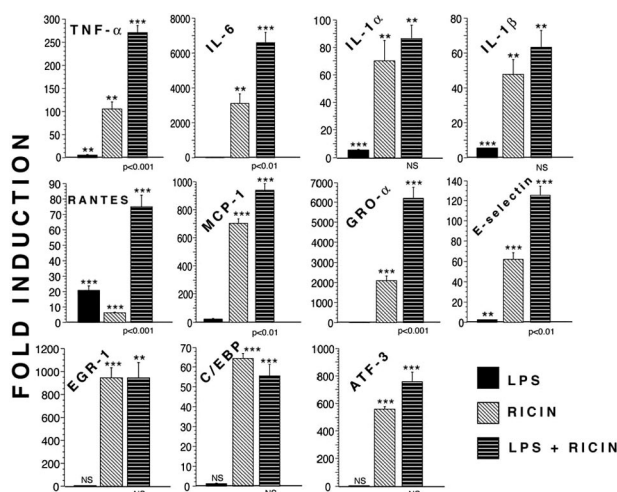


Figure 9. Gene expression in mouse kidneys after administration of LPS, ricin, and LPS plus ricin. Mice received 12 μ g of ricin/100 g body weight i.v., LPS 10 μ g i.p., or both. Each group contains triplicate mice, which were sacrificed at 24 hours for harvesting kidneys. Real-time RT-PCR analyses were performed on RNA extracted from harvested organs. *P* values are as follows: *, *P* < 0.05; **, *P* < 0.01; ***, *P* < 0.001; and NS, nonsignificant. Asterisks above bars show comparison between treatments and controls; *P* values shown below bars of LPS plus ricin treatment show the comparison of this treatment to ricin alone. Error bars represent SEM.

responses that regulate transcription of proinflammatory cytokines and chemokines. Yet to date, the proinflammatory actions of ricin have been primarily overlooked in comparison to the attention given to the ability of ricin to trigger the inhibition of protein synthesis. In intestinal epithelial cells Stx and ricin activate the ribotoxic stress response, which leads to the elevation of genes encoding chemokines and cytokines via the activation of JNK and p38 MAPK.^{62–64} Only recently has it been recognized that mechanisms of action different from the mere inhibition of translation are operational in the clinical conditions triggered by poisoning with Stx-1 and Stx-2, two homologous proteins that have intracellular activities identical to those of ricin.²¹ These toxins are produced by *E. coli* bacteria and, in humans, lead to development of HUS, a condition characterized by a severe inflammatory response. The current study represents the first attempt in a murine model system to characterize the signaling intermediates and transcriptional products that contribute to the consequences of ricin intoxication.

As previously suggested, monocyte/macrophages may play a pivotal role in the pathogenesis of Stx-induced HUS.¹⁷ These cells represent an important source of cytokines, including TNF- α and IL-1, which may additionally sensitize other cells, such as endothelial cells, to the effects of Stx.^{65,66} Increased numbers of macrophages have been detected in glomeruli of patients with Stx-induced HUS compared to control patients.^{67,68} In a mouse model of Stx-induced HUS in mice, Stx cytotoxicity was reduced after the depletion of the hepatic and splenic macrophages.⁶⁹ We therefore chose to study the effects of ricin on the inflammatory response in macrophages. Ricin strongly induced the activation of the JNK and p38 MAPK, as well as ERK 1/2, and produced a dose-dependent increase in TNF- α mRNA. The finding

that ricin induced the secretion of TNF- α only at ricin concentrations less than 1 μ g/ml (Figure 1d) may be attributed to a partial block in protein synthesis at these lower ricin concentrations. These studies demonstrate that the effects of ricin on the activation of MAPK family members and the strong transcriptional activation of TNF- α and other genes (Figure 2) occurs at concentrations of ricin that only partially interfere with the translation of proteins. The ability of ricin-intoxicated cells to translate mRNAs induced in those cells may explain our *in vivo* results in which intravascularly administered ricin produced an increase in plasma-borne TNF- α , IL-6, and IL-1 β proteins. These studies indicate that, despite the decreased translation that may occur in some cell types *in vivo*, the high levels of induced mRNAs corresponding to some proinflammatory genes (Table 3) may be sufficient to drive the increased production of proinflammatory mediators.

Experiments performed on RAW 264.7 macrophages revealed that the activation of MAPK family members were required to mediate the accumulation of RNA encoded by multiple proinflammatory mediators and transcription factors (Figure 2). Although many of the genes investigated were differentially dependent on ERK, JNK, or p38 MAPK for ricin's ability to induce the accumulation of RNAs that they encode, blockade of all three MAPK families invariably reduced the accumulation of RNA to basal or near-basal levels. The high representation of transcription factors among the group of RNAs whose expression was increased by ricin in the Affymetrix microarray analysis (Tables 2 and 3) supports the notion that an important function of ricin in mediating proinflammatory responses occurs by the induced expression of genes that encode transcription factors. The documented involvement of activated ERK, JNK, and p38 MAPK in mediating the activation of transcription factors by direct phosphorylation^{10,11,70} suggests that MAPKs participate in the transcriptional activation of transcription factors and, ultimately, of proinflammatory mediators (cytokines, chemokines, and cell surface molecules) that are associated with the proinflammatory effects of ricin. Additionally, ERK and p38 MAPK have been identified as mediators of cytokine release via their ability to activate proteases such as TNF- α -converting enzyme (TACE) that direct the shedding of TNF- α and perhaps other cell surface-tethered cytokines.^{71–74} Thus, ricin may additionally induce the proteolytic cleavage and release of cytokines whose transcription ricin has previously directed. In addition, the p38 MAPK pathway also contributes to the inducible expression of mRNA encoded by inflammatory genes through the stabilization of transcripts that contain a 3'-UTR AU-rich motif,^{75,76} commonly associated with RNAs that encode proinflammatory mediators, thereby suggesting that ricin also may induce the accumulation of RNAs through pathways that do not involve transcriptional activation.

In this report, we studied a murine model of ricin intoxication that could be used not only as a model to study the inflammatory response that is triggered after the intravenous administration of ricin toxin but also to study the pathogenic mechanisms that participate in develop-

ment of HUS in humans. Mice that were injected with ricin developed thrombocytopenia, hemolytic anemia, and renal failure. Even though we failed to detect histological evidence of glomerular thrombosis on the H&E staining, we observed extensive deposition of fibrin(ogen) in the glomerular capillary loops and peritubular capillaries by using immunohistochemical staining with an anti-fibrin(ogen) antibody (Figures 3 and 4). We failed to detect histopathological evidence of necrosis of the tubular epithelium, a common feature of animal models of HUS after administration of Stx.⁷⁷ This feature of Stx-induced pathology in animal models contrasts with the typical absence of tubular necrosis in human HUS.

It has been concluded that Stx is the main etiological factor in the pathogenesis of HUS.¹⁵ Yet, attempts to reproduce the complete clinical presentation of the human HUS in animals others than baboons⁷⁸ after administration of Stx alone have not been successful, suggesting that other factors participate in the pathogenesis of HUS.^{15,57,79} It has been reported that LPS/endotoxin, which is a major inflammatory mediator produced by gram-negative bacteria, is an important factor in the development of the disease.⁸⁰ LPS initiates a cellular inflammatory response mediated by the toll-like receptor TLR-4,^{81,82} through activation of the p38 MAPK and/or activation of the NF- κ B pathways, with subsequent transcriptional activation of genes that are involved in the inflammatory response.⁸³ Twenty-four hours after its administration, LPS alone was relatively ineffective in elevating the levels of RNA encoded by proinflammatory genes, compared with administration of ricin alone (Figure 9). This result could be explained by the transient nature of LPS actions on the SAPK cascade compared to the sustained activation of the SAPKs produced by ricin.⁵⁻⁹ Additionally, we analyzed the RNA levels encoded by proinflammatory genes 24 hours after the administration of LPS. It is possible that we failed to detect the ability of LPS alone to induce expression of cytokines because of its rapid onset and rapid return to basal levels. Interestingly, the co-administration of LPS and ricin resulted in a synergistic increase in RNAs encoded by some cytokines (TNF- α and IL-6) and chemokines (RANTES, MCP-1, and GRO- α). However, the administration of LPS failed to augment the expression of mRNAs that encode several transcriptional regulators (EGR-1, C/EBP β , and ATF3) and the proinflammatory cytokine IL-1 (Figure 9). LPS signals the activation of both NF- κ B and SAPK cascades,⁸³ in contrast to ricin that activates only the SAPK cascade in cell cultures (unpublished results). This distinction may be responsible for the ability of LPS to synergize with ricin in augmenting the responsiveness of genes encoding cytokines and chemokines that contain binding sites for both NF- κ B and AP-1 proteins in their regulatory regions. It has been suggested that LPS and Stx together may increase the abundance of certain proinflammatory gene transcripts through alterations in the transcriptional and posttranscriptional control mechanisms.⁸⁴

Evidence suggests that ricin and Stx exert their pathological effects by interacting directly with the endothelium. Several reports demonstrate that, despite improve-

ments in the chemical structure of ricin-containing immunotoxins, the development of vascular leak syndrome limits the application of ricin as a component in the therapy of cancer.⁸⁵ It is suspected that vascular leak syndrome results from the direct interaction of ricin with endothelial cells and/or macrophages and that this interaction is responsible for the injury of the endothelium by ricin.²⁸ The endothelium also appears to play an essential role in the pathogenesis of HUS.¹⁵ It is well known that the injury of endothelial cells contributes to the development of microvascular thrombosis,^{15,17,80} a consequence of HUS that has been difficult to achieve in Stx-induced animal models.^{69,86-88} The immunohistochemical staining shown in Figure 4 demonstrates remarkable deposition of fibrinogen/fibrin in the renal microvasculature after the administration of ricin *in vivo*. Endothelial damage, the adhesion and aggregation of platelets, and the deposition of fibrin are involved in the formation of thrombotic lesions that are a determining step in the outcome of HUS patients. After their activation, endothelial cells actively participate in the development of the inflammatory response, either by secretion of inflammatory mediators (IL-1, IL-6, IL-8, MCP-1, GRO- α , RANTES, and so forth) and/or by expressing on their surface adhesion proteins (eg, P-selectin, E-selectin, ICAM-1, VCAM-1, and so forth) that trigger the recruitment of leukocytes.⁸⁹ After the administration of ricin *in vivo*, we demonstrated by immunohistochemical localization that activation of the MAP kinase superfamily members occurred in endothelial cells in different organs (data not shown). The direct activation of MAPKs in response to ricin in the endothelium could modulate the inflammatory responses of these cells by activating the transcription of genes that encode inflammatory mediators and the subsequent translation of these gene products. By using real-time RT-PCR, we found that, after the injection of ricin *in vivo*, the expression of mRNA that encodes E-selectin was increased several fold compared to sham-injected mice (Figure 9). The finding that a peak in the expression of the mRNA that encodes the E-selectin gene occurred earlier than the expression of mRNAs encoding most of the other inflammatory cytokines and chemokines that were analyzed (Figure 7) suggests an early involvement and activation of the endothelium in response to ricin *in vivo*.

In this report, we performed Affymetrix microarray analyses to identify RNAs whose abundance was increased in response to systemic administration of ricin *in vivo* (Table 3). The profile of genes whose RNA products were increased after the intravenous administration of ricin showed similarity with previously published Affymetrix microarray data from lung tissue after intratracheal application of ricin.⁹⁰ Ricin as an efficient inducer of an inflammatory response *in vivo* potentially induced mRNAs that encode transcriptional regulators, several chemokine and cytokine genes, and a variety of adhesion proteins that are known to participate in interactions between leukocytes and the activated endothelial cells in the context of an active inflammatory response (eg, the selectins, ICAM-1, and syndecan-1). The profile of cytokine/chemokine genes that were induced by ricin *in vivo* included IL-1 β , IL-6, CCL2 (MCP-1), and CXCL-1 (Gro-

α). This profile of gene expression shares similarity with profiles of genes that previously have been shown to be up-regulated in patients with HUS.^{24,25,68,91–95}

EGR1 was one of the transcription factors whose RNA was greatly increased in abundance after the administration of ricin. EGR1 is up-regulated after mitogenic stimulation,⁹⁶ during radiation injuries,⁹⁷ hypoxia,⁹⁸ and during the induction of apoptosis.⁹⁹ It has been reported that induced expression of EGR1 is closely related to an increased proliferation of mesangial cells in a model of experimental mesangio-proliferative glomerulonephritis.¹⁰⁰ Downstream target genes of EGR-1 are platelet-derived growth factor-A (PDGF-A) and PDGF-B,^{101,102} transforming growth factor- β (TGF- β),¹⁰¹ intercellular adhesion molecule-1 (ICAM-1),^{103,104} TNF- α ,¹⁰¹ and M-CSF.¹⁰⁵ The expression of several of these EGR-1-dependent mRNAs, such as PDGF-B, ICAM-1, and M-CSF were up-regulated in animals that received ricin (Table 3).

After the administration of ricin *in vivo*, we also detected increased expression of genes that encode several members of the coagulation cascade and fibrinolytic pathway. It has been suggested that the microvascular thrombosis observed in HUS is related to abnormalities in the coagulation and fibrinolytic pathways.^{106–108} The role of fibrinolysis in the pathogenesis of HUS is still controversial. Some reports demonstrate the activation of fibrinolytic pathways in HUS patients,^{109,110} whereas others have not confirmed this activation.¹¹¹ In our studies after ricin application *in vivo*, we found an increased expression of genes that encode factor I, factor III, and factor X (all members of the coagulation cascade), and PAI-1 (a physiological inhibitor of the plasminogen activators that participates in the fibrinolytic pathway). Our data suggest that ricin may trigger increased expression of molecules that participate in the coagulation cascade and fibrinolysis *in vivo*, although verification by detection of the translated products awaits further experimentation.

Experiments that used real-time RT-PCR to quantify RNAs (Figures 7 and 9) demonstrated that in many cases the Affymetrix microarrays severely underestimated the increased levels of RNA induced by ricin (compare Table 2 with Figures 7 and 9). In other experiments, we have used the same RNA in both Affymetrix microarray and real-time RT-PCR experiments and have verified that the Affymetrix data frequently underestimates the level of induction by ricin (unpublished). It is well known that microarrays exhibit a limited dynamic range that is unsuitable for the measurement of very large changes in RNA abundance, such as that which occurred after the administration of ricin.

In view of differences in the cell type-specific distribution of Gb3 molecules between humans and other species, it has been difficult to recapitulate the development of HUS after administration of Stx in animal models.⁸⁰ Many factors contribute to the etiology of HUS in humans, including the distribution of receptors on cell types, potential modulation of receptor expression by cytokines, and toxin-specific differences in the intracellular trafficking of receptors that leads to delivery of their enzymatic moieties to the cytosol. Despite these differences, the intracellular molecular targets of ricin and Stx are identi-

cal.⁶⁴ Foster and Tesh⁶⁵ reported that Stx-1 induces the activation of p38 MAPK and JNK in human macrophages and that blockade of p38 MAPK activation reduced the production of TNF- α . These investigators concluded that Stx triggers the ribotoxic stress response in macrophages, and that macrophages may be the possible source of cytokine production in the kidneys. The present communication extends these observations to ricin-treated macrophages and further demonstrates that administration of ricin to mice recapitulates many of the features of HUS and provides a mechanistic basis for approaching the development of the disease. The availability of transgenic and knockout mice that have altered expression of genes that encode cytokines, chemokines, surface adhesion molecules, and proteins involved in thrombosis and fibrinolysis should facilitate further investigations into the etiology of HUS. Animal and preclinical studies have demonstrated the efficacy of a variety of selective small molecule inhibitors of p38 MAPK in reducing the expression of TNF- α , IL-1, and IL-6 in arthritic and other inflammatory diseases, and some compounds have reached phase II and III trials.³⁶ The administration of ricin to mice may facilitate the development of similar therapeutic strategies aimed at ameliorating the life-threatening consequences of HUS or reducing the potentially lethal consequences of ricin toxicity should ricin be used as an agent of warfare.

Acknowledgments

We thank Olga Ryabinina, Thanh-Hoai Dinh, and Remy Choi for important technical contributions.

References

1. Franz DR, Jaax JK: Ricin toxin. Textbook of Military Medicine, Part 1. Warfare, Weaponry, and the Casualty: Medical Aspects of Chemical and Biological Warfare. Edited by FR Sidell, ET Takfuji, DR Franz. Washington, Office of the Surgeon General, Department of the Army, 1997, pp 631–642
2. Smallshaw JE, Firan A, Fulmer JR, Ruback SL, Ghetie V, Vitetta ES: A novel recombinant vaccine which protects mice against ricin intoxication. *Vaccine* 2002, 20:3422–3427
3. Crompton R, Gall D: Georgi Markov—death in a pellet. *Med Leg J* 1980, 48:51–62
4. Barbieri L, Battelli MG, Stirpe F: Ribosome-inactivating proteins from plants. *Biochim Biophys Acta* 1993, 1154:237–282
5. Iordanov MS, Pribnow D, Magun JL, Dinh TH, Pearson JA, Chen SL, Magun BE: Ribotoxic stress response: activation of the stress-activated protein kinase JNK1 by inhibitors of the peptidyl transferase reaction and by sequence-specific RNA damage to the alpha-sarcin/ricin loop in the 28S rRNA. *Mol Cell Biol* 1997, 17:3373–3381
6. Iordanov MS, Magun BE: Loss of cellular K⁺ mimics ribotoxic stress. Inhibition of protein synthesis and activation of the stress kinases SEK1/MKK4, stress-activated protein kinase/c-Jun NH2-terminal kinase 1, and p38/HOG1 by palytoxin. *J Biol Chem* 1998, 273:3528–3534
7. Iordanov MS, Pribnow D, Magun JL, Dinh TH, Pearson JA, Magun BE: Ultraviolet radiation triggers the ribotoxic stress response in mammalian cells. *J Biol Chem* 1998, 273:15794–15803
8. Iordanov MS, Magun BE: Different mechanisms of c-Jun NH(2)-terminal kinase-1 (JNK1) activation by ultraviolet-B radiation and by oxidative stressors. *J Biol Chem* 1999, 274:25801–25806
9. Iordanov MS, Choi RJ, Ryabinina OP, Dinh TH, Bright RK, Magun BE:

- The UV (ribotoxic) stress response of human keratinocytes involves the unexpected uncoupling of the Ras-extracellular signal-regulated kinase signaling cascade from the activated epidermal growth factor receptor. *Mol Cell Biol* 2002, 22:5380–5394
10. Waskiewicz AJ, Cooper JA: Mitogen and stress response pathways: MAP kinase cascades and phosphatase regulation in mammals and yeast. *Curr Opin Cell Biol* 1995, 7:798–805
 11. Kyriakis JM, Avruch J: Mammalian mitogen-activated protein kinase signal transduction pathways activated by stress and inflammation. *Physiol Rev* 2001, 81:807–869
 12. Bingen A, Creppy EE, Gut JP, Dirheimer G, Kirn A: The Kupffer cell is the first target in ricin-induced hepatitis. *J Submicrosc Cytol* 1987, 19:247–256
 13. Taylor CM, Williams JM, Lote CJ, Howie AJ, Thewles A, Wood JA, Milford DV, Raafat F, Chant I, Rose PE: A laboratory model of toxin-induced hemolytic uremic syndrome. *Kidney Int* 1999, 55:1367–1374
 14. Gerber A, Karch H, Allerberger F, Verwey HM, Zimmerhackl LB: Clinical course and the role of Shiga toxin-producing *Escherichia coli* infection in the hemolytic-uremic syndrome in pediatric patients, 1997–2000, in Germany and Austria: a prospective study. *J Infect Dis* 2002, 186:493–500
 15. Paton JC, Paton AW: Pathogenesis and diagnosis of Shiga toxin-producing *Escherichia coli* infections. *Clin Microbiol Rev* 1998, 11:450–479
 16. Ruggerenti P, Noris B, Remuzzi G: Thrombotic microangiopathy, hemolytic uremic syndrome, and thrombotic thrombocytopenic purpura. *Kidney Int* 2001, 60:831–846
 17. Proulx F, Seidman EG, Karpman D: Pathogenesis of Shiga toxin-associated hemolytic uremic syndrome. *Pediatr Res* 2001, 50:163–171
 18. O'Brien AD, Holmes RK: Shiga and Shiga-like toxins. *Microbiol Rev* 1987, 51:206–220
 19. Olsnes S, Kozlov JV: Ricin. *Toxicon* 2001, 39:1723–1728
 20. Cohen A, Hannigan GE, Williams BR, Lingwood CA: Roles of globotriosyl- and galabiosylceramide in verotoxin binding and high affinity interferon receptor. *J Biol Chem* 1987, 262:17088–17091
 21. Sandvig K, Grimmer S, Lauvrak SU, Torgersen ML, Skretting G, van Deurs B, Iversen TG: Pathways followed by ricin and Shiga toxin into cells. *Histochem Cell Biol* 2002, 117:131–141
 22. Rowe PC, Orrbine E, Wells GA, McLaine PN: Epidemiology of hemolytic-uremic syndrome in Canadian children from 1986 to 1988. The Canadian Pediatric Kidney Disease Reference Centre. *J Pediatr* 1991, 119:218–224
 23. Thorpe CM: Shiga toxin-producing *Escherichia coli* infection. *Clin Infect Dis* 2004, 38:1298–1303
 24. Litalien C, Proulx F, Mariscalco MM, Robitaille P, Turgeon JP, Orrbine E, Rowe PC, McLaine PN, Seidman E: Circulating inflammatory cytokine levels in hemolytic uremic syndrome. *Pediatr Nephrol* 1999, 13:840–845
 25. Yamamoto T, Isokawa S, Miyata H, Yoshioka K: Evaluation of thrombomodulin and tumor necrosis factor- α levels in patients with hemolytic uremic syndrome caused by enterohemorrhagic *Escherichia coli* O157:H7 infection. *Nippon Jinzo Gakkai Shi* 1999, 41:60–64
 26. Lopez EL, Contrini MM, Devoto S, de Rosa MF, Grana MG, Genero MH, Canepa C, Gomez HF, Cleary TG: Tumor necrosis factor concentrations in hemolytic uremic syndrome patients and children with bloody diarrhea in Argentina. *Pediatr Infect Dis J* 1995, 14:594–598
 27. Kreitman RJ: Immunotoxins in cancer therapy. *Curr Opin Immunol* 1999, 11:570–578
 28. Frankel AE, Tagge EP, Willingham MC: Clinical trials of targeted toxins. *Semin Cancer Biol* 1995, 6:307–317
 29. Engert A, Sausville EA, Vitetta E: The emerging role of ricin A-chain immunotoxins in leukemia and lymphoma. *Curr Top Microbiol Immunol* 1998, 234:13–33
 30. Hochberg Y, Benjamini Y: More powerful procedures for multiple significance testing. *Stat Med* 1990, 9:811–818
 31. Chen CC, Wang JK: p38 but not p44/42 mitogen-activated protein kinase is required for nitric oxide synthase induction mediated by lipopolysaccharide in RAW 264.7 macrophages. *Mol Pharmacol* 1999, 55:481–488
 32. Chakravorty D, Kato Y, Sugiyama T, Koide N, Mu MM, Yoshida T, Yokochi T: Inhibition of caspase 3 abrogates lipopolysaccharide-induced nitric oxide production by preventing activation of NF- κ B and c-Jun NH2-terminal kinase/stress-activated protein kinase in RAW 264.7 murine macrophage cells. *Infect Immun* 2001, 69:1315–1321
 33. Yamasaki S, Nakashima T, Kawakami A, Miyashita T, Tanaka F, Ida H, Migita K, Origuchi T, Eguchi K: Cytokines regulate fibroblast-like synovial cell differentiation to adipocyte-like cells. *Rheumatology (Oxford)* 2004, 43:448–452
 34. Higuchi S, Tamura T, Oda T: Cross-talk between the pathways leading to the induction of apoptosis and the secretion of tumor necrosis factor- α in ricin-treated RAW 264.7 cells. *J Biochem (Tokyo)* 2003, 134:927–933
 35. Hassoun E, Wang X: Ricin-induced toxicity in the macrophage J774A.1 cells: the role of TNF- α and the modulation effects of TNF- α polyclonal antibody. *J Biochem Mol Toxicol* 2000, 14:95–101
 36. Kumar S, Boehm J, Lee JC: p38 MAP kinases: key signalling molecules as therapeutic targets for inflammatory diseases. *Nat Rev Drug Discov* 2003, 2:717–726
 37. Saklatvala J, Dean J, Clark A: Control of the expression of inflammatory response genes. *Biochem Soc Symp* 2003, 70:95–106
 38. Lee JC, Kumar S, Griswold DE, Underwood DC, Votta BJ, Adams JL: Inhibition of p38 MAP kinase as a therapeutic strategy. *Immunopharmacology* 2000, 47:185–201
 39. Herlaar E, Brown Z: p38 MAPK signalling cascades in inflammatory disease. *Mol Med Today* 1999, 5:439–447
 40. Angel P, Karin M: The role of Jun, Fos and the AP-1 complex in cell-proliferation and transformation. *Biochim Biophys Acta* 1991, 1072:129–157
 41. Guha M, O'Connell MA, Pawlinski R, Hollis A, McGovern P, Yan SF, Stern D, Mackman N: Lipopolysaccharide activation of the MEK-ERK1/2 pathway in human monocytic cells mediates tissue factor and tumor necrosis factor α expression by inducing Elk-1 phosphorylation and Egr-1 expression. *Blood* 2001, 98:1429–1439
 42. Shi L, Kishore R, McMullen MR, Nagy LE: Lipopolysaccharide stimulation of ERK1/2 increases TNF- α production via Egr-1. *Am J Physiol* 2002, 282:C1205–C1211
 43. Droin NM, Pinkoski MJ, Dejardin E, Green DR: Egr family members regulate nonlymphoid expression of Fas ligand, TRAIL, and tumor necrosis factor during immune responses. *Mol Cell Biol* 2003, 23:7638–7647
 44. Moake JL: Thrombotic thrombocytopenic purpura and the hemolytic uremic syndrome. *Arch Pathol Lab Med* 2002, 126:1430–1433
 45. Hosack DA, Dennis Jr G, Sherman BT, Lane HC, Lempicki RA: Identifying biological themes within lists of genes with EASE. *Genome Biol* 2003, 4:R70
 46. Thomson S, Mahadevan LC, Clayton AL: MAP kinase-mediated signalling to nucleosomes and immediate-early gene induction. *Semin Cell Dev Biol* 1999, 10:205–214
 47. Liang G, Wolfgang CD, Chen BP, Chen TH, Hai T: ATF3 gene. Genomic organization, promoter, and regulation. *J Biol Chem* 1996, 271:1695–1701
 48. Kool J, Hamdi M, Cornelissen-Steijger P, van der Eb AJ, Terleth C, van Dam H: Induction of ATF3 by ionizing radiation is mediated via a signaling pathway that includes ATM, Nibrin1, stress-induced MAP kinases and ATF-2. *Oncogene* 2003, 22:4235–4242
 49. Inoue K, Zama T, Kamimoto T, Aoki R, Ikeda Y, Kimura H, Hagiwara M: TNF α -induced ATF3 expression is bidirectionally regulated by the JNK and ERK pathways in vascular endothelial cells. *Genes Cells* 2004, 9:59–70
 50. Bradley MN, Zhou L, Smale ST: C/EBP β regulation in lipopolysaccharide-stimulated macrophages. *Mol Cell Biol* 2003, 23:4841–4858
 51. Hanlon M, Sturgill TW, Sealy L: ERK2- and p90(Rsk2)-dependent pathways regulate the CCAAT/enhancer-binding protein- β interaction with serum response factor. *J Biol Chem* 2001, 276:38449–38456
 52. Wang Q, Doerschuk CM: The signaling pathways induced by neutrophil-endothelial cell adhesion. *Antioxid Redox Signal* 2002, 4:39–47
 53. Vestweber D, Blanks JE: Mechanisms that regulate the function of the selectins and their ligands. *Physiol Rev* 1999, 79:181–213
 54. Therrien M, Wong AM, Rubin GM: CNK, a RAF-binding multidomain protein required for RAS signaling. *Cell* 1998, 95:343–353
 55. Ceci JD, Patriotis CP, Tsatsanis C, Makris AM, Kovatch R, Swing DA, Jenkins NA, Tschlis PN, Copeland NG: Tpl-2 is an oncogenic kinase that is activated by carboxy-terminal truncation. *Genes Dev* 1997, 11:688–700

56. Turgeon B, Lang BF, Meloche S: The protein kinase ERK3 is encoded by a single functional gene: genomic analysis of the ERK3 gene family. *Genomics* 2002, 80:673–680
57. Remuzzi G, Ruggenenti P: The hemolytic uremic syndrome. *Kidney Int* 1995, 48:2–19
58. Coratelli P, Buongiorno E, Passavanti G: Endotoxemia in hemolytic uremic syndrome. *Nephron* 1988, 50:365–367
59. Karpman D, Connell H, Svensson M, Scheutz F, Alm P, Svanborg C: The role of lipopolysaccharide and Shiga-like toxin in a mouse model of *Escherichia coli* O157:H7 infection. *J Infect Dis* 1997, 175:611–620
60. Barrett TJ, Potter ME, Wachsmuth IK: Bacterial endotoxin both enhances and inhibits the toxicity of Shiga-like toxin II in rabbits and mice. *Infect Immun* 1989, 57:3434–3437
61. Ikeda M, Ito S, Honda M: Hemolytic uremic syndrome induced by lipopolysaccharide and Shiga-like toxin. *Pediatr Nephrol* 2004, 5:485–489
62. Smith WE, Kane AV, Campbell ST, Acheson DW, Cochran BH, Thorpe CM: Shiga toxin 1 triggers a ribotoxic stress response leading to p38 and JNK activation and induction of apoptosis in intestinal epithelial cells. *Infect Immun* 2003, 71:1497–1504
63. Thorpe CM, Smith WE, Hurley BP, Acheson DW: Shiga toxins induce, superinduce, and stabilize a variety of C-X-C chemokine mRNAs in intestinal epithelial cells, resulting in increased chemokine expression. *Infect Immun* 2001, 69:6140–6147
64. Thorpe CM, Hurley BP, Lincicome LL, Jacewicz MS, Keusch GT, Acheson DW: Shiga toxins stimulate secretion of interleukin-8 from intestinal epithelial cells. *Infect Immun* 1999, 67:5985–5993
65. Foster GH, Tesh VL: Shiga toxin 1-induced activation of c-Jun NH(2)-terminal kinase and p38 in the human monocytic cell line THP-1: possible involvement in the production of TNF-alpha. *J Leukoc Biol* 2002, 71:107–114
66. Shimada O, Ishikawa H, Tosaka-Shimada H, Atsumi S: Exocytotic secretion of toxins from macrophages infected with *Escherichia coli* O157. *Cell Struct Funct* 1999, 24:247–253
67. Inward CD, Howie AJ, Fitzpatrick MM, Rafaat F, Milford DV, Taylor CM: Renal histopathology in fatal cases of diarrhoea-associated haemolytic uraemic syndrome. *British Association for Paediatric Nephrology. Pediatr Nephrol* 1997, 11:556–559
68. van Setten PA, van Hinsbergh VW, van den Heuvel LP, Preyers F, Dijkman HB, Assmann KJ, van der Velden TJ, Monnens LA: Monocyte chemoattractant protein-1 and interleukin-8 levels in urine and serum of patients with hemolytic uremic syndrome. *Pediatr Res* 1998, 43:759–767
69. Palermo MS, Alves Rosa MF, Van Rooijen N, Isturiz MA: Depletion of liver and splenic macrophages reduces the lethality of Shiga toxin-2 in a mouse model. *Clin Exp Immunol* 1999, 116:462–467
70. Marshall CJ: MAP kinase kinase kinase, MAP kinase kinase and MAP kinase. *Curr Opin Genet Dev* 1994, 4:82–89
71. Fan H, Derynck R: Ectodomain shedding of TGF-alpha and other transmembrane proteins is induced by receptor tyrosine kinase activation and MAP kinase signaling cascades. *EMBO J* 1999, 18:6962–6972
72. Gechtman Z, Alonso JL, Raab G, Ingber DE, Klagsbrun M: The shedding of membrane-anchored heparin-binding epidermal-like growth factor is regulated by the Raf/mitogen-activated protein kinase cascade and by cell adhesion and spreading. *J Biol Chem* 1999, 274:28828–28835
73. Montero JC, Yuste L, Diaz-Rodriguez E, Esparis-Ogando A, Pandiella A: Mitogen-activated protein kinase-dependent and -independent routes control shedding of transmembrane growth factors through multiple secretases. *Biochem J* 2002, 363:211–221
74. Rizoli SB, Rotstein OD, Kapus A: Cell volume-dependent regulation of L-selectin shedding in neutrophils. A role for p38 mitogen-activated protein kinase. *J Biol Chem* 1999, 274:22072–22080
75. Kontoyiannis D, Pasparakis M, Pizarro TT, Cominelli F, Kollias G: Impaired on/off regulation of TNF biosynthesis in mice lacking TNF AU-rich elements: implications for joint and gut-associated immunopathologies. *Immunity* 1999, 10:387–398
76. Winzen R, Kracht M, Ritter B, Wilhelm A, Chen CY, Shyu AB, Muller M, Gaestel M, Resch K, Holtmann H: The p38 MAP kinase pathway signals for cytokine-induced mRNA stabilization via MAP kinase-activated protein kinase 2 and an AU-rich region-targeted mechanism. *EMBO J* 1999, 18:4969–4980
77. Tesh VL, Burris JA, Owens JW, Gordon VM, Wadolkowski EA, O'Brien AD, Samuel JE: Comparison of the relative toxicities of Shiga-like toxins type I and type II for mice. *Infect Immun* 1993, 61:3392–3402
78. Taylor Jr FB, Tesh VL, DeBault L, Li A, Chang AC, Kosanke SD, Pysher TJ, Siegler RL: Characterization of the baboon responses to Shiga-like toxin: descriptive study of a new primate model of toxic responses to Stx-1. *Am J Pathol* 1999, 154:1285–1299
79. Ashkenazi S: Role of bacterial cytotoxins in hemolytic uremic syndrome and thrombotic thrombocytopenic purpura. *Annu Rev Med* 1993, 44:11–18
80. Ray PE, Liu XH: Pathogenesis of Shiga toxin-induced hemolytic uremic syndrome. *Pediatr Nephrol* 2001, 16:823–839
81. Poltorak A, He X, Smirnova I, Liu MY, Van Huffel C, Du X, Birdwell D, Alejos E, Silva M, Galanos C, Freudenberg M, Ricciardi-Castagnoli P, Layton B, Beutler B: Defective LPS signaling in C3H/HeJ and C57BL/10ScCr mice: mutations in Tlr4 gene. *Science* 1998, 282:2085–2088
82. Qureshi ST, Lariviere L, Leveque G, Clermont S, Moore KJ, Gros P, Malo D: Endotoxin-tolerant mice have mutations in Toll-like receptor 4 (Tlr4). *J Exp Med* 1999, 189:615–625
83. Kaisho T, Akira S: Toll-like receptors as adjuvant receptors. *Biochim Biophys Acta* 2002, 1589:1–13
84. Harrison LM, van Haaften WC, Tesh VL: Regulation of proinflammatory cytokine expression by Shiga toxin 1 and/or lipopolysaccharides in the human monocytic cell line THP-1. *Infect Immun* 2004, 72:2618–2627
85. Vitetta ES: Immunotoxins and vascular leak syndrome. *Cancer J* 2000, 6(Suppl 3):S218–S224
86. Rutjes NW, Binnington BA, Smith CR, Maloney MD, Lingwood CA: Differential tissue targeting and pathogenesis of verotoxins 1 and 2 in the mouse animal model. *Kidney Int* 2002, 62:832–845
87. Palermo M, Alves-Rosa F, Rubel C, Fernandez GC, Fernandez-Alonso G, Alberto F, Rivas M, Isturiz M: Pretreatment of mice with lipopolysaccharide (LPS) or IL-1beta exerts dose-dependent opposite effects on Shiga toxin-2 lethality. *Clin Exp Immunol* 2000, 119:77–83
88. Tesh VL, Samuel JE, Perera LP, Sharefkin JB, O'Brien AD: Evaluation of the role of Shiga and Shiga-like toxins in mediating direct damage to human vascular endothelial cells. *J Infect Dis* 1991, 164:344–352
89. Krishnaswamy G, Kelley J, Yerra L, Smith JK, Chi DS: Human endothelium as a source of multifunctional cytokines: molecular regulation and possible role in human disease. *J Interferon Cytokine Res* 1999, 19:91–104
90. DaSilva L, Cote D, Roy C, Martinez M, Duniho S, Pitt ML, Downey T, Dertzbaugh M: Pulmonary gene expression profiling of inhaled ricin. *Toxicol* 2003, 41:813–822
91. Proulx F, Turgeon JP, Litalien C, Mariscalco MM, Robitaille P, Seidman E: Inflammatory mediators in *Escherichia coli* O157:H7 hemorrhagic colitis and hemolytic-uremic syndrome. *Pediatr Infect Dis J* 1998, 17:899–904
92. van de Kar NC, Sauerwein RW, Demacker PN, Grau GE, van Hinsbergh VW, Monnens LA: Plasma cytokine levels in hemolytic uremic syndrome. *Nephron* 1995, 71:309–313
93. Murata A, Shimazu T, Yamamoto T, Taenaka N, Nagayama K, Honda T, Sugimoto H, Monden M, Matsuura N, Okada S: Profiles of circulating inflammatory- and anti-inflammatory cytokines in patients with hemolytic uremic syndrome due to *E. coli* O157 infection. *Cytokine* 1998, 10:544–548
94. Andreoli SP: The pathophysiology of the hemolytic uremic syndrome. *Curr Opin Nephrol Hypertens* 1999, 8:459–464
95. Proulx F, Toledano B, Phan V, Clermont MJ, Mariscalco MM, Seidman EG: Circulating granulocyte colony-stimulating factor, C-X-C, and C-C chemokines in children with *Escherichia coli* O157:H7 associated hemolytic uremic syndrome. *Pediatr Res* 2002, 52:928–934
96. Sukhatme VP, Kartha S, Toback FG, Taub R, Hoover RG, Tsai-Morris CH: A novel early growth response gene rapidly induced by fibroblast, epithelial cell and lymphocyte mitogens. *Oncogene Res* 1987, 1:343–355
97. Hallahan DE, Sukhatme VP, Sherman ML, Virudachalam S, Kufe D, Weichselbaum RR: Protein kinase C mediates x-ray inducibility of nuclear signal transducers EGR1 and JUN. *Proc Natl Acad Sci USA* 1991, 88:2156–2160
98. Yan SF, Lu J, Zou YS, Soh-Won J, Cohen DM, Buttrick PM, Cooper DR, Steinberg SF, Mackman N, Pinsky DJ, Stern DM: Hypoxia-associated induction of early growth response-1 gene expression. *J Biol Chem* 1999, 274:15030–15040

99. Nair P, Muthukkumar S, Sells SF, Han SS, Sukhatme VP, Rangnekar VM: Early growth response-1-dependent apoptosis is mediated by p53. *J Biol Chem* 1997, 272:20131–20138
100. Carl M, Akagi Y, Weidner S, Isaka Y, Imai E, Rupperecht HD: Specific inhibition of Egr-1 prevents mesangial cell hypercellularity in experimental nephritis. *Kidney Int* 2003, 63:1302–1312
101. Silverman ES, Collins T: Pathways of Egr-1-mediated gene transcription in vascular biology. *Am J Pathol* 1999, 154:665–670
102. Khachigian LM, Collins T: Inducible expression of Egr-1-dependent genes. A paradigm of transcriptional activation in vascular endothelium. *Circ Res* 1997, 81:457–461
103. Maltzman JS, Carman JA, Monroe JG: Role of EGR1 in regulation of stimulus-dependent CD44 transcription in B lymphocytes. *Mol Cell Biol* 1996, 16:2283–2294
104. Maltzman JS, Carmen JA, Monroe JG: Transcriptional regulation of the *Icam-1* gene in antigen receptor- and phorbol ester-stimulated B lymphocytes: role for transcription factor EGR1. *J Exp Med* 1996, 183:1747–1759
105. Srivastava S, Weitzmann MN, Kimble RB, Rizzo M, Zahner M, Milbrandt J, Ross FP, Pacifici R: Estrogen blocks M-CSF gene expression and osteoclast formation by regulating phosphorylation of Egr-1 and its interaction with Sp-1. *J Clin Invest* 1998, 102:1850–1859
106. Robson WL, Leung AK, Kaplan BS: Hemolytic-uremic syndrome. *Curr Probl Pediatr* 1993, 23:16–33
107. Richardson SE, Karmali MA, Becker LE, Smith CR: The histopathology of the hemolytic uremic syndrome associated with verocytotoxin-producing *Escherichia coli* infections. *Hum Pathol* 1988, 19:1102–1108
108. Drummond KN: Hemolytic uremic syndrome—then and now. *N Engl J Med* 1985, 312:116–118
109. Proesmans W, Geet CV: Fibrinolysis in the hemolytic uremic syndrome. *Pediatr Nephrol* 2002, 17:871–874
110. Van Geet C, Proesmans W, Arnout J, Vermeylen J, Declerck PJ: Activation of both coagulation and fibrinolysis in childhood hemolytic uremic syndrome. *Kidney Int* 1998, 54:1324–1330
111. Chandler WL, Jelacic S, Boster DR, Ciol MA, Williams GD, Watkins SL, Igarashi T, Tarr PI: Prothrombotic coagulation abnormalities preceding the hemolytic-uremic syndrome. *N Engl J Med* 2002, 346:23–32